SIRT1 contributes to telomere maintenance and augments global homologous recombination

Jose A. Palacios,[1] Daniel Herranz,[2] Maria Luigia De Bonis,[1,3] Susana Velasco,[2] Manuel Serrano,[2] and Maria A. Blasco[1]

[1]Telomeres and Telomerase Group and [2]Tumor Suppression Group, Molecular Oncology Program, Spanish National Cancer Centre, Madrid E-28029, Spain
[3]Istituto di Ricovero e Cura a Carattere Scientifico, Oncology Reference Center of Basilicata, Rionero in Vulture (PZ) 85028, Italy

Yeast Sir2 deacetylase is a component of the silent information regulator (SIR) complex encompassing Sir2/Sir3/Sir4. Sir2 is recruited to telomeres through Rap1, and this complex spreads into subtelomeric DNA via histone deacetylation. However, potential functions at telomeres for SIRT1, the mammalian orthologue of yeast Sir2, are less clear. We studied both loss of function (*SIRT1* deficient) and gain of function (*SIRT1*^{super}) mouse models. Our results indicate that SIRT1 is a positive regulator of telomere length in vivo and attenuates telomere shortening associated with aging, an effect dependent on telomerase activity. Using chromatin immunoprecipitation assays, we find that SIRT1 interacts with telomeric repeats in vivo. In addition, SIRT1 overexpression increases homologous recombination throughout the entire genome, including telomeres, centromeres, and chromosome arms. These findings link SIRT1 to telomere biology and global DNA repair and provide new mechanistic explanations for the known functions of SIRT1 in protection from DNA damage and some age-associated pathologies.

Introduction

Telomeres are specialized nucleoprotein structures that protect the ends of eukaryotic chromosomes from unscheduled DNA repair reactions and degradation (Chan and Blackburn, 2002; de Lange, 2005). In vertebrates, telomeres consist of TTAGGG repeats bound by a specialized multiprotein complex known as *shelterin*, which has fundamental roles in the regulation of telomere length and protection (Liu et al., 2004; de Lange, 2005). Because of the intrinsic inability of the DNA replication machinery to copy the end of linear molecules, and to endogenous DNA end–degrading activities, telomeres become progressively shorter after every cell division cycle (Harley et al., 1990; Blasco, 2005).

Telomere repeats are generated by a ribonucleoprotein reverse transcriptase known as telomerase (Greider and Blackburn, 1985); however, its abundance and activity in adult tissues is not sufficient to compensate for the progressive telomere attrition that occurs with aging (Collins and Mitchell, 2002). In humans, several studies have described an inverse correlation between telomere length and age in a variety of tissues and between telomere length and certain age-associated diseases (Cawthon et al., 2003; Panossian et al., 2003; Ogami et al., 2004; Canela et al., 2007). Also, factors that may decrease longevity, such as psychological stress or obesity, are proposed to negatively impact on telomerase activity and telomere length (Epel et al., 2004; Valdes et al., 2005). In the absence of telomerase, telomeres can be maintained by a recombination-dependent mechanism (Dunham et al., 2000) known as alternative lengthening of telomeres (ALT; McEachern et al., 2000), which involves DNA repair proteins such as the Mre11–Rad50–Nbs1 and SMC5–SMC6–MMS21 complexes (Jiang et al., 2005; Potts and Yu, 2007).

Silent information regulator 2 (Sir2) family of proteins is a group of NAD^+-dependent deacetylases/ADP-ribosyltransferases (type III histone deacetylase) initially discovered in yeast and are identified as key regulators of health span and lifespan in yeast and other organisms (Haigis and Guarente, 2006). Yeast Sir2 functions encompass (a) repression of gene expression at the silent mating type loci HML and HMR (Klar et al., 1979; Rine et al., 1979) (b) to suppress recombination at the ribosomal

Correspondence to Maria A. Blasco: mblasco@cnio.es

Abbreviations used in this paper: ALT, alternative lengthening of telomeres; auf, arbitrary units of fluorescence; ChIP, chromatin immunoprecipitation; CO-FISH, chromosome orientation FISH; CR, calorie restriction; DSB, double-strand break; iPS, induced pluripotent stem; MEF, mouse embryonic fibroblast; MTS, multiple telomeric signals; Q-FISH, quantitative FISH; SCE, sister chromatid exchange; SFE, signal-free end; TRF, telomere restriction fragment.

The Rockefeller University Press $30.00
J. Cell Biol. Vol. 191 No. 7 1299–1313
www.jcb.org/cgi/doi/10.1083/jcb.201005160

DNA locus, thus preventing generation of toxic ribosomal DNA circles (Sinclair and Guarente, 1997), and (c) to maintain the heterochromatic state of telomeres (Bedalov et al., 2001; Xu et al., 2007).

Mammals have seven (SIRT1–7) known sirtuins, of which SIRT1 is the closest and best-characterized mammalian orthologue of yeast Sir2 (Brachmann et al., 1995; Frye, 1999). SIRT1 deacetylase activity has been involved in chromatin remodeling, gene silencing, and the DNA damage response (Kim and Um, 2008; Cantó and Auwerx, 2009; Milner, 2009). Furthermore, mounting evidence has connected SIRT1 to stress responses in mammals (Abdelmohsen et al., 2007; Wang et al., 2007; Westerheide et al., 2009). In particular, SIRT1 is recruited to the chromatin upon different DNA damage insults, where it favors efficient repair of double-strand breaks (DSBs) by homologous recombination (Oberdoerffer et al., 2008). In this regard, SIRT1 physically interacts and deacetylates the WRN helicase (Vaitiekunaite et al., 2007; Kahyo et al., 2008; Li et al., 2008; Law et al., 2009), in this manner modulating homologous recombination–dependent DSB DNA repair (Uhl et al., 2010). SIRT1 also targets Nbs1, a regulatory subunit of the Mre11–Rad50–Nbs1 complex (Yuan and Seto, 2007; Yuan et al., 2007). SIRT1-mediated Nbs1 deacetylation specifically inhibits Nbs1 phosphorylation and modulates its activity in intra–S phase checkpoint induction (Kastan and Lim, 2000; Lim et al., 2000). Together, these findings suggest a potential role of SIRT1 in the regulation of DNA repair pathways.

Much attention has recently been given to the role of SIRT1 in metabolic tissues, such as the liver, skeletal muscle, and adipose tissues, where it deacetylates a range of substrates, including key metabolic regulators PGC1α, UCP2, NFκB, and Foxo proteins, which in turn have pronounced effects on glucose homeostasis, insulin secretion, and lipid homeostasis (Liang et al., 2009). Among other metabolic effects, SIRT1 is known to participate in the activation of gluconeogenic genes and to increase both hepatic glucose output during calorie restriction (CR) and reverse cholesterol transport and fat mobilization in white adipose tissue (Brooks and Gu, 2009). We have previously generated mice that contain additional copies of the *SIRT1* gene under the control of its natural regulatory elements and that express threefold SIRT1 in a homogenous and systemic manner across all tissues, known as *SIRT1*^{super} mice (Pfluger et al., 2008). These mice are protected from physiological damage produced by exposure to a high fat diet. In addition, *SIRT1*^{super} mice are protected from DNA damage and liver carcinogenesis and show decreased signs of aging, including decreased expression of the aging-associated gene p16Ink4a (Herranz et al., 2010).

In yeast, Sir2, together with Sir3 and Sir4, is recruited to telomeres through Rap1, and this complex spreads along subtelomeric sequences enforcing transcriptional silencing (Perrod and Gasser, 2003; Bühler and Gasser, 2009). A Rap1-like protein is conserved in both human and fission yeast (Konig et al., 1996; Li et al., 2000; Park et al., 2002). However, human Rap1 lacks the DNA-interacting Myb domain and does not bind telomeric repeats. Other Myb box–related-containing proteins in mammals such as TRF2 bind directly to telomeric DNA repeats (Broccoli et al., 1997) and mediate the association of human Rap1 to telomeres (de Lange, 2009; Takai et al., 2010). A potential role of SIRT1 at mammalian telomeres is, therefore, less clear. More recently, SIRT1 depletion has been shown to cause telomere dysfunction (El Ramy et al., 2009). Interestingly, activation of SIRT1 with resveratrol produces an increase in extrachromosomal telomeric DNA and in colocalization of telomeric TRF1 with WRN helicase and BRCA1 in cells that elongate telomeres using ALT (Rusin et al., 2009).

In this study, we set to understand a potential role of mammalian SIRT1 in telomere biology by studying both loss of function (*SIRT1*-deficient mice) and gain of function (*SIRT1*^{super} mice) mouse models (Cheng et al., 2003; Pfluger et al., 2008). Our results indicate that mammalian SIRT1 interacts with the mouse telomeric repeats and acts as a positive regulator of telomere length in vivo by significantly attenuating telomere shortening associated with mouse aging. In addition, we find an important role of SIRT1 in promoting recombination at different chromosomal regions, including telomeres, centromeres, and chromosome arms. These findings link SIRT1 to telomeres and provide new mechanistic explanations for the known roles of augmented SIRT1 expression in protection from DNA damage and in prevention from some age-associated pathologies.

Results

SIRT1 levels influence telomere length in mouse embryonic fibroblasts (MEFs)

To address a potential role of SIRT1 in telomere length maintenance, we performed both telomere restriction fragment (TRF) analysis and metaphase telomere quantitative FISH (Q-FISH) on MEFs derived from either *SIRT1*-deficient or *SIRT1*^{super} mice and their corresponding wild-type controls. We have previously shown that *SIRT1*^{super} MEFs have a threefold increase in SIRT1 expression compared with wild-type controls (Pfluger et al., 2008; Herranz et al., 2010). *SIRT1*^{super} MEFs showed a modest but significant increase in mean telomere length compared with wild-type MEFs both by TRF and Q-FISH analyses (Fig. 1 A; and Fig. S1, A and B). Q-FISH analysis further indicated that increased telomere length in *SIRT1*^{super} MEFs is accompanied by a significant decrease of signal-free ends (SFEs) or chromosome ends with undetectable telomere signals and by a decrease in the proportion of short telomeres (<30 kb) and an increase in the proportion of long telomeres (>80 kb; Fig. 1 B). These results indicate that elevated SIRT1 expression leads to improved telomere length maintenance in cultured primary MEFs. In turn, *SIRT1*-deficient MEFs showed significantly shorter telomeres compared with wild-type MEFs as determined both by Q-FISH and TRF analyses (Fig. 1 C; and Fig. S1, A and B). Shorter mean telomere length in *SIRT1*$^{-/-}$ MEFs was accompanied by a significant increase in the proportion of short telomeres and a decrease in the proportion of long telomeres (Fig. 1 D). To confirm whether the observed effects were specifically associated with the SIRT1 protein, wild-type and *SIRT1*$^{-/-}$ MEFs were transfected with a SIRT1-coding plasmid (for SIRT1 expression levels see Fig. S2, A and B) and evaluated its effect on telomere length by Q-FISH analysis. Both *SIRT1*$^{+/+}$ and *SIRT1*$^{-/-}$ MEFs

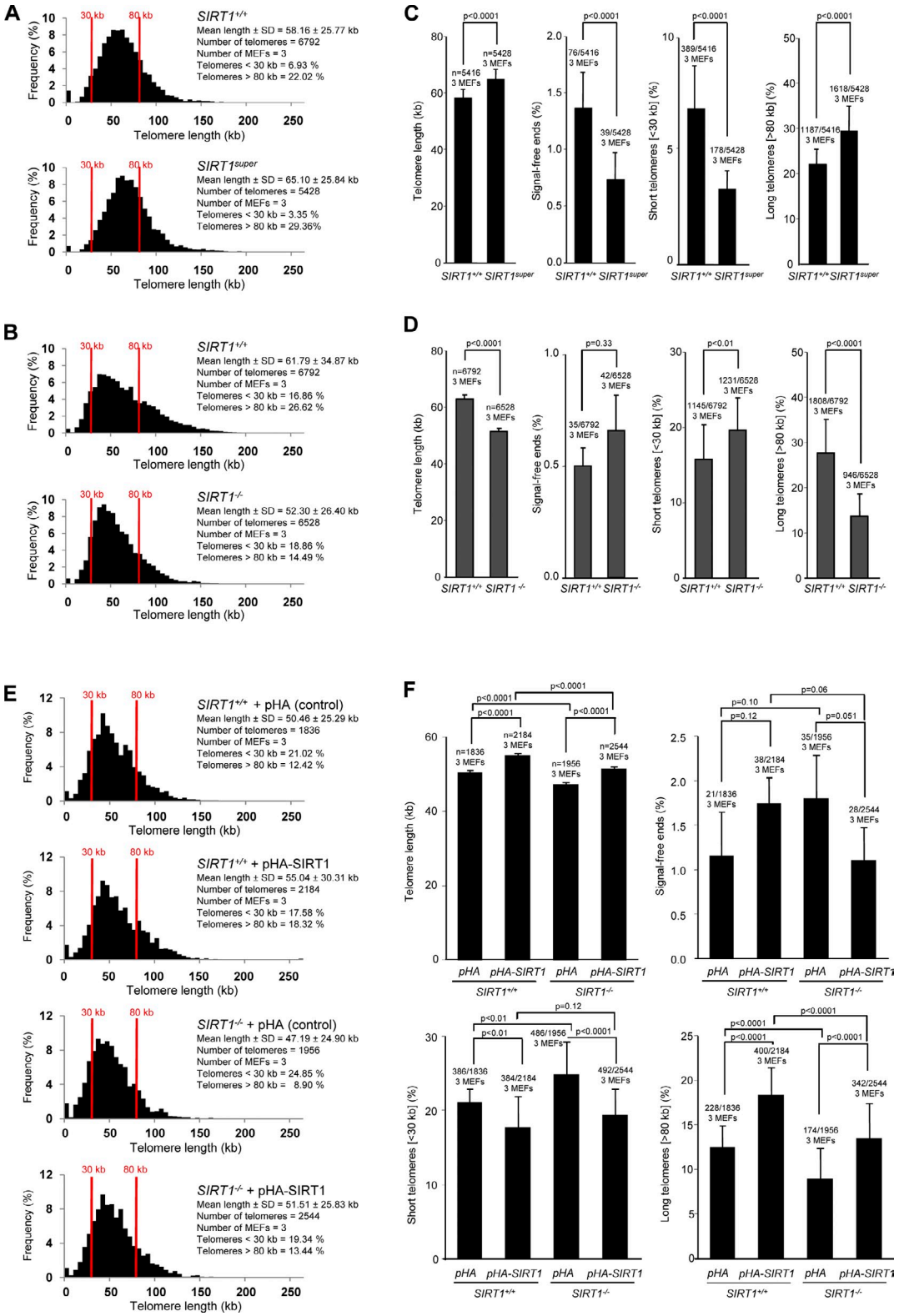

Figure 1. **Increased SIRT1 expression leads to longer telomeres, whereas SIRT1 deficiency results in telomere shortening in primary MEFs.** (A) Telomere length frequency distribution (Q-FISH) in metaphase spreads from *SIRT1*$^{+/+}$ and *SIRT1*^{super} primary (passage 2) MEFs. (B) Telomere length frequency distribution (Q-FISH) in metaphase spreads from *SIRT1*$^{+/+}$ and *SIRT1*$^{-/-}$ primary (passage 2) MEFs. (C and D) Mean telomere length, percentage of SFEs, percentage of short telomeres (<30 kb), and percentage of long telomeres (>80 kb) in primary MEFs from the indicated genotypes. (E) Telomere length frequency distribution (Q-FISH) in metaphase spreads from *SIRT1*$^{+/+}$ and *SIRT1*$^{-/-}$ primary (passage 2) MEFs transfected with pHA-SIRT1 (pCruz-HA-SIRT1) and pHA (pCruz-HA) plasmids. (F) Mean telomere length, percentage of SFEs, percentage of short telomeres (<30 kb), and percentage of long telomeres (>80 kb) in primary MEFs from the indicated genotypes. SEM, number of MEFs, and the number of telomeres used for analysis are shown for each genotype. Student's *t* test was used in the case of mean telomere intensity; otherwise, the Fisher exact test was used for statistical calculations. P-values are indicated.

transfected with the SIRT1 plasmid showed an increase in telomere length compared with cells transfected with the control plasmid (Fig. 1 E). In all cases, increased telomere length was accompanied by a significant decrease in the proportion of short telomeres (<30 kb) and an increase in the proportion of long telomeres (>80 kb); an almost significant decrease in SFEs was also observed in the SIRT1-tranfected *SIRT1*$^{-/-}$ MEFs (Fig. 1 F). Together, the analyses of gain of function and loss of function MEFs for SIRT1 strongly suggest a role for the mammalian homologue of yeast Sir2 in telomere length maintenance in vivo.

Increased SIRT1 expression attenuates telomere erosion with age in adult tissues

Given the presence of longer telomeres in *SIRT1*^{super} MEFs, we wondered whether increased SIRT1 expression also improved telomere length maintenance in the context of adult mouse tissues. We have recently shown that SIRT1 overexpression in mice has significant beneficial effects on liver function (Pfluger et al., 2008; Herranz et al., 2010). Thus, we set to measure telomere length in liver sections from age- and sex-matched *SIRT1*^{super} and *SIRT*$^{+/+}$ littermates using telomere Q-FISH. Telomere length analysis of the hepatic parenchyma of 2-yr-old *SIRT1*^{super} mice showed a significant increase in mean telomere length compared with wild-type controls (Fig. 2 A). Longer telomeres in the liver of old *SIRT1*^{super} mice were accompanied by a significant increase in the proportion of very long telomeres (>80 arbitrary units of fluorescence [auf]) and a significant reduction in the proportion of short telomeres (<60 auf; Fig. 2 B). Furthermore, supporting a role for SIRT1 in telomere maintenance, liver sections from 2-yr-old *SIRT1*$^{-/-}$ mice showed significantly shorter telomeres than those of age-matched *SIRT1*$^{+/+}$ controls in the hepatic parenchyma (Fig. 2 D). In concordance with the results in MEFs, shorter mean telomere length was accompanied by a significant increase in the proportion of very short telomeres (<100 auf) and by a significant decrease in the proportion of very long telomeres (>120 auf; Fig. 2 E). The same analysis was conducted in kidney sections (both in renal glomeruli and tubules) from 2-mo- and 2-yr-old mice. Mean telomere length decreased both in the glomeruli and tubules from 2-yr-old mice compared with 2-mo-old wild-type mice, which is in agreement with our previous observations showing telomere shortening associated with old age in many mouse tissues (Flores et al., 2008). Notably, this trend is not observed in *SIRT1*^{super} mice, where 2-yr-old mice showed longer telomeres compared with 2-mo-old mice (Fig. 2 G). Longer telomeres in the kidney of *SIRT1*^{super} mice were accompanied by an increase in the proportion of cells with long telomeres and a reduction in the proportion of cells with short telomeres in *SIRT1*^{super} mice in both age groups (Fig. 2, G and H). In particular, although wild-type kidneys showed an increase in the percentage of cells with short telomeres in 2-yr-old mice compared with 2-mo-old mice, which was concomitant with a decrease in the percentage of cells with very long telomeres (Fig. 2 H), these changes were not observed in kidneys from *SIRT1*^{super} mice (Fig. 2 H). Together, these results suggest that a moderate increase in SIRT1 expression (threefold) has beneficial effects on telomere length maintenance during aging. This finding is in agreement with the fact that *SIRT1*^{super} mice are protected from some age-related diseases such as hepatic steatosis, insulin resistance, liver cancer associated with metabolic syndrome, and osteoporosis (Pfluger et al., 2008; Herranz et al., 2010).

SIRT1 effects on telomere length are largely dependent on telomerase activity

In most eukaryotes, telomeres are maintained by telomerase, a reverse transcription that adds telomeric repeats de novo after every cell division cycle, in this manner counteracting for the incomplete DNA replication of telomeres caused by the end replication problem (Collins and Mitchell, 2002; Chan and Blackburn, 2004). To address the mechanisms by which cells and tissues from SIRT1-overexpressing mice show improved telomere length maintenance, we first set to measure telomerase activity by using the in vitro TRAP assay (see Materials and methods). As shown in Fig. 3 (A and B), in vitro telomerase activity was similar in wild-type and *SIRT1*^{super} MEFs, indicating that increased SIRT1 expression does not significantly affect telomerase in vitro activity.

Next, we addressed whether longer telomeres in *SIRT1*^{super} MEFs were dependent on the presence of a proficient telomerase complex. To this end, we generated *SIRT1*^{super} mice simultaneously deficient for the essential telomerase RNA component (*Terc*) gene and measured telomere length in first-generation *SIRT1*^{super}*;Terc*$^{+/+}$, *SIRT1*^{super}*;Terc*$^{-/-}$, *SIRT1*$^{+/+}$*;Terc*$^{+/+}$, and *SIRT1*$^{+/+}$*;Terc*$^{-/-}$ MEFs. Southern blot–based TRF analysis confirmed longer telomeres in *SIRT1*^{super} MEFs compared with wild-type controls in a telomerase-proficient *Terc*$^{+/+}$ background (Fig. 3, C and D). *Terc* deficiency resulted in significant telomere shortening in both the *SIRT1*$^{+/+}$ and *SIRT1*^{super} backgrounds, indicating similar rates of telomere erosion in the absence of telomerase activity. Further analysis using the more-sensitive Q-FISH technique confirmed a significant increase in SFEs and in the frequency of short telomeres (<20 kb) both in *SIRT1*$^{+/+}$*;Terc*$^{-/-}$ and *SIRT1*^{super}*;Terc*$^{-/-}$ MEFs (Fig. 3, E and F), again indicating that telomerase deficiency causes similar rates of telomere erosion independently of SIRT1 amounts. Q-FISH analysis also indicated that *SIRT1*^{super}*;Terc*$^{-/-}$ MEFs showed a similar mean telomere length to that of *SIRT1*$^{+/+}$*; Terc*$^{-/-}$ controls, again suggesting that longer telomeres in *SIRT1*^{super} MEFs are dependent on the presence of telomerase activity. Interestingly, the percentage of SFEs and cells with short telomeres was significantly increased in *SIRT1*^{super}*;Terc*$^{-/-}$ MEFs compared with *SIRT1*$^{+/+}$*;Terc*$^{-/-}$ controls, suggesting that augmented SIRT1 expression may accelerate telomere loss when in the absence of telomerase activity. In line with this, survival curves of a small cohort of *SIRT1*^{super}*;Terc*$^{+/+}$, *SIRT1*$^{+/+}$*;Terc*$^{+/+}$, *SIRT1*^{super}*;Terc*$^{-/-}$, and *SIRT1*$^{+/+}$*;Terc*$^{-/-}$ mice show that *SIRT1*^{super}*;Terc*$^{-/-}$ mice have a significant decreased survival when compared with *SIRT1*$^{+/+}$*;Terc*$^{-/-}$ mice (Fig. S5), which further suggests a negative effect of increased SIRT1 expression in the context of telomerase deficiency. Together, these results suggest that maintenance of longer telomeres in *SIRT1*^{super} MEFs requires the presence of a proficient telomerase complex.

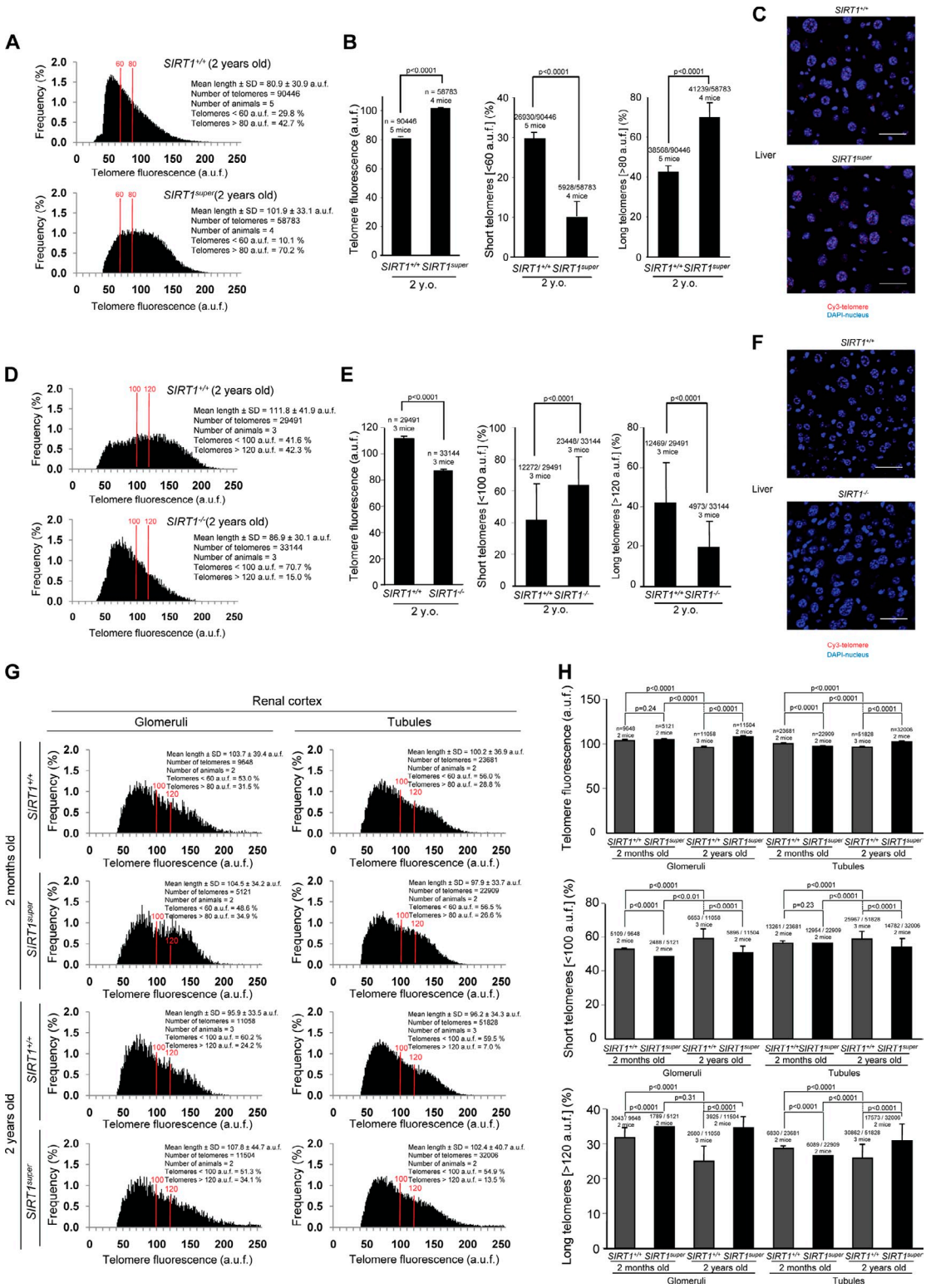

Figure 2. **Increased SIRT1 expression improves telomere length maintenance with increasing age in *SIRT1*^{super} mice.** (A and D, left) Telomere fluorescence frequency distribution as determined by Q-FISH on liver sections from mice of the indicated genotypes. (C and F) Representative images of telomere Q-FISH on liver sections from *SIRT1*^{super} and *SIRT1*$^{+/+}$ mice, where DAPI nuclear staining is shown in blue and telomere signal in red. (B) Mean telomere length in auf, percentage of short telomeres (<60 auf), and percentage of long telomeres (>80 auf) are shown. (E) Mean telomere length in auf, percentage of short telomeres (<100 auf), and percentage of long telomeres (>120 auf) are shown. (G) Telomere fluorescence frequency distribution (Q-FISH) of glomeruli and tubules in kidney sections from mice of the indicated age and genotype. (H) Mean telomere fluorescence, percentage of short telomeres (<100 auf), and percentage of long telomeres (>120 auf) are shown. Note that telomere fluorescence decreases with age in kidney glomeruli and tubules indicative of telomere shortening, whereas this shortening does not occur in *SIRT1*^{super} mice. SEM, the number of animals, and telomere signals used for the analysis are shown for each genotype. Student's *t* test was used in the case of the mean telomere intensity; otherwise, the Fisher exact test was used for statistical calculations. P-values are indicated. Bars, 100 µm.

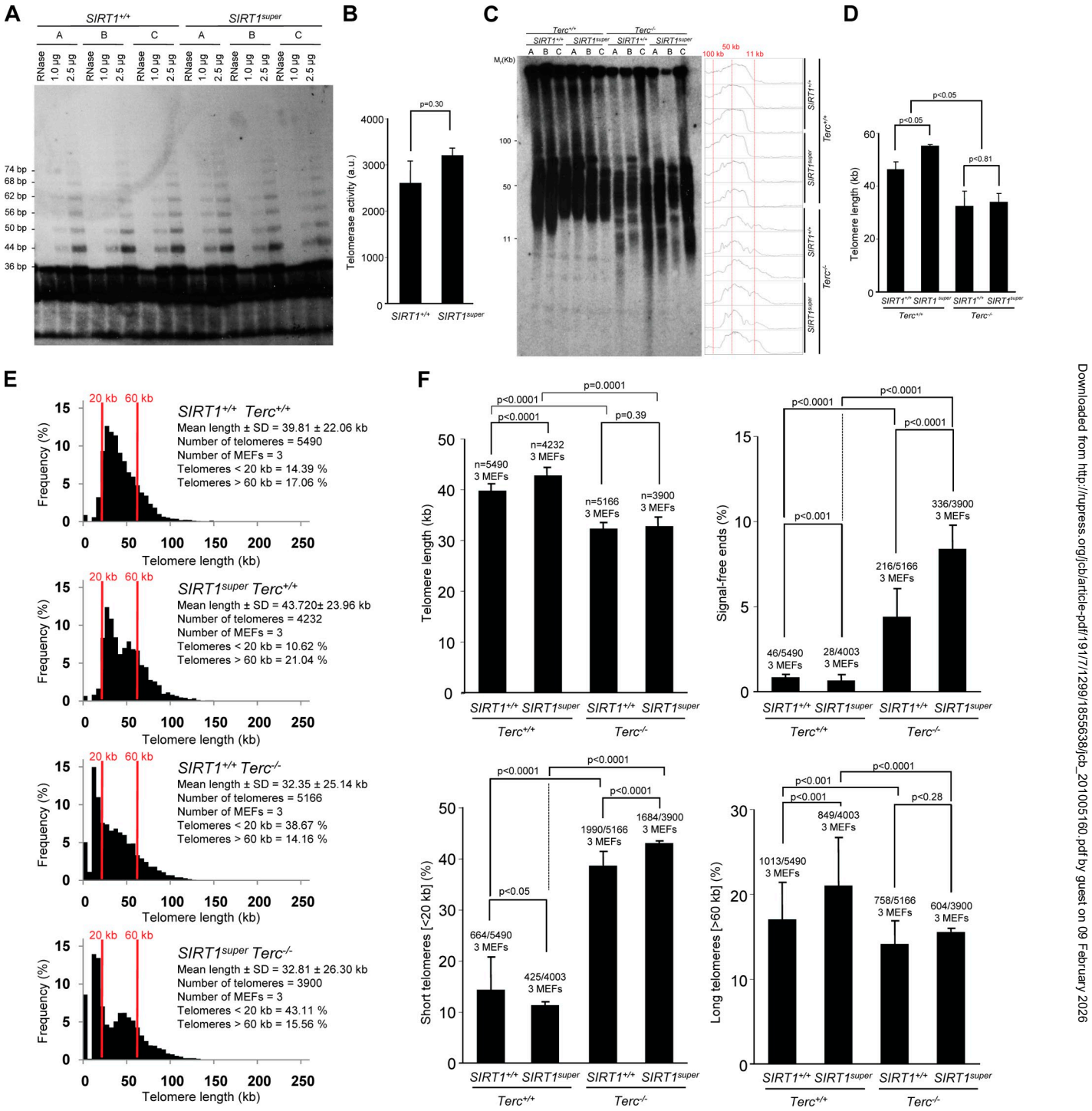

Figure 3. **SIRT1 effects on telomere length are largely dependent on a proficient telomerase complex.** (A) Telomerase in vitro TRAP activity is similar in *SIRT1*^{super} and wild-type primary (passage 2) MEFs (n = 3). A representative TRAP gel is shown for illustrative purposes. (B) Quantification of telomerase TRAP activity is expressed in arbitrary units (au). Extracts were pretreated (+) or not (−) with RNase as a negative control. n = number of TRAP assays from a total of three MEF cultures per genotype. (C) TRF analysis of primary (passage 2) MEFs of the indicated genotypes (n = 3). Note accumulation of small-size telomere fragments in the *Terc*-deficient genotypes independently of SIRT1 status. (D) Mean telomere length in MEFs of the indicated genotypes as determined by TRF is shown. SEM and number of MEFs used for the analysis are indicated for each genotype. The Student's t test was used for statistical calculations, and p-values are indicated. (E) Telomere length frequency distribution (Q-FISH) in metaphase spreads from primary MEFs of the indicated genotypes. All MEFs used are littermates. (F) Mean telomere length, percentage of SFEs, percentage of short telomeres (<20 kb), and percentage of long telomeres (>60 kb) are shown. SEM and number of telomeres used for the analysis are shown for each genotype. Student's t test was used in the case of mean telomere length and TRAP assay; otherwise, the Fisher exact test was used for statistical calculations. P-values are indicated. Note a similar increase in SFEs and in the percentage of short telomeres in wild-type and *SIRT1*^{super} MEFs in the context of telomerase deficiency (*Terc*$^{-/-}$). Note that mean telomere length values are not directly comparable with those shown in Fig. 1 because of the fact that they correspond to independent experiments not performed in parallel and fluorescence intensity may vary between different experiments.

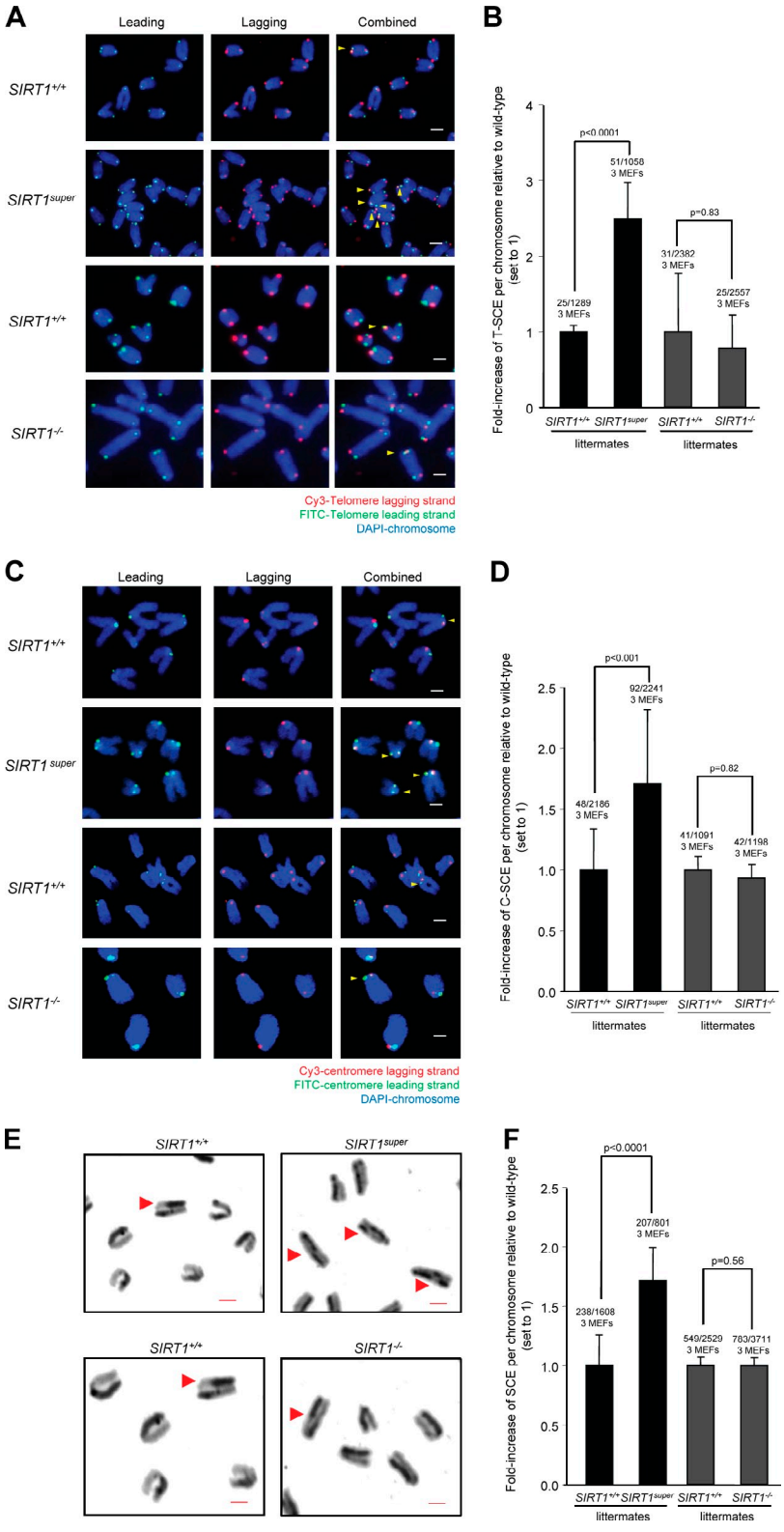

Figure 4. **SIRT1-increased expression results in higher recombination frequencies at telomeres, centromeres, and chromosome arms.** (A) Representative telomere CO-FISH images of chromosomes from primary (passage 2) MEFs of the indicated genotypes showing increased recombination events at telomeres (T-SCE) in *SIRT1*^{super} MEFs. Lagging strand is shown in red, leading strand in green, and DAPI staining in blue. Yellow arrowheads indicate occurrence of T-SCE. (B) Quantification of sister telomere recombination events (T-SCE) expressed as a fold increase with respect to wild-type MEFs (set to 1). (C) Representative centromere CO-FISH images of chromosomes from primary (passage 2) MEFs showing increased recombination at centromeres (C-SCE) in *SIRT1*^{super} MEFs. Lagging strand is shown in red, leading strand in green, and DAPI staining in blue. Yellow arrowheads indicate occurrence of C-SCE. (D) Quantification of the centromere recombination events (C-SCE) expressed as a fold increased of wild-type MEFs (set to 1). SEM, number of recombination events, and total number of analyzed MEFs and chromosomes are indicated. Fisher exact test was used for statistical analysis, and p-values are indicated. (E) Representative images of chromosomes from primary (passage 2) MEFs showing increased SCE at chromosome arms in *SIRT1*^{super} MEFs. Red arrowheads indicate SCE events. (F) Quantification of global recombination events (SCE) expressed as a fold increased of wild-type MEFs (set to 1). SEM, number of recombination events, and total number of analyzed MEFs and chromosomes are indicated. Fisher exact test was used for statistical analysis, and p-values are indicated. Bars, 1 µm.

Increased SIRT1 expression augments homologous recombination at telomeres, centromeres, and chromosome arms

Telomere maintenance by ALT relies on recombination events between telomeric sequences. To address whether SIRT1 influences telomere recombination frequencies, we performed chromosome orientation FISH (CO-FISH) on *SIRT1*^{super} and *SIRT1*$^{-/-}$ MEFs and their respective wild-type controls, which measures the frequency of sister chromatid exchanges (SCEs) specifically at the telomeric repeats (T-SCE; Bailey et al., 1996). Strikingly, MEFs overexpressing SIRT1 showed a significant increase in the frequency of SCEs at telomeres compared with

their wild-type controls (Fig. 4, A and B), suggesting that increased SIRT1 expression favors telomeric recombination. Interestingly, *SIRT1* abrogation in MEFs did not significantly affect T-SCEs frequencies compared with wild-type controls. Together, these results suggest that SIRT1 gain of function significantly augments homologous recombination between telomeric sequences but that SIRT1 activity is not essential to mediate these events. Notably, increased telomere recombination may be responsible for accelerated telomere loss of *SIRT1*^{super} MEFs compared with controls when a telomerase-deficient background is present (Fig. 3 E). In particular, homologous recombination at telomeric repeats can occur at multiple points, leading to an unequal exchange of telomeric repeats, thus generating chromosomes with unequal telomere lengths including short and long telomeres (Bailey et al., 2004; Blagoev and Goodwin, 2008).

Next, we set to determine whether the effect of increased SIRT1 expression on homologous recombination was specific of telomeric regions or reflected a global role of SIRT1 in favoring homologous recombination throughout the genome. To this end, we measured SCE events both at centromeric repeats (C-SCE; Jaco et al., 2008) and chromosome arms (SCE; see Materials and methods). As shown in Fig. 4 (C and D), *SIRT1*^{super} MEFs showed increased frequencies of C-SCE, whereas *SIRT1*$^{-/-}$ MEFs showed normal frequencies compared with wild-type MEFs. SCE frequencies at chromosome arms were also significantly elevated in *SIRT1*^{super} MEFs compared with wild-type controls or *SIRT1*$^{-/-}$ MEFs, confirming an impact of increased SIRT1 expression on global recombination frequencies (Fig. 4, E and F).

SIRT1 deficiency triggers a DNA damage response at chromosome ends

As *SIRT1* deficiency in MEFs results in shorter mean telomere length compared with wild-type MEFs and SIRT1 overexpression significantly increases SCE frequencies, we wondered whether SIRT1 abrogation or SIRT1 overexpression could lead to increased damage at telomeres. γ-H2AX foci have been previously shown to indicate the presence of DNA DSBs, including those associated with critically short and dysfunctional telomeres, also known as TIFs (d'Adda di Fagagna et al., 2003; Takai et al., 2003). SIRT1 overexpression in *SIRT1*^{super} MEFs did not significantly increase the occurrence of TIFs when compared with their respective wild-type controls (Fig. 5, A and B). In contrast, *SIRT1*-deficient MEFs showed a significant increase in the proportion of cells with more than three TIFs compared with the wild-type controls (Fig. 5, A and B). These results suggest that although increased SIRT1 expression has no deleterious effects on telomere function, *SIRT1* deficiency results in significant telomere dysfunction.

SIRT1 prevents telomere fragility

To further explore a putative role of SIRT1 in telomere protection, we performed metaphase Q-FISH analysis with a telomeric probe on *SIRT1*^{super} and *SIRT1*$^{-/-}$ MEFs and their respective wild-type controls. *SIRT1*$^{-/-}$ MEFs showed a significantly increased proportion of chromosome ends with multiple telomeric signals (MTS) (Fig. 6, A, C, and D), a type of aberration recently

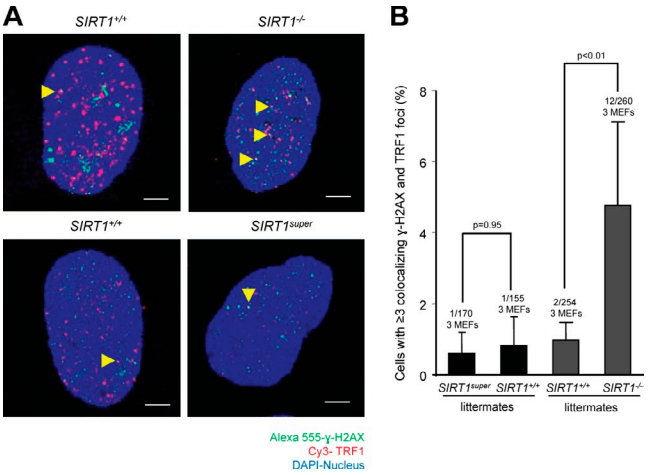

Figure 5. **SIRT1 deficiency leads to increased telomere damage in primary MEFs.** (A) Representative images of TRF1 (red) and γ-H2AX (green) immunofluorescence. Colocalization events indicate occurrence of TIFs (yellow arrowheads). (B) Quantification of cells with more than three TIFs in primary MEFs of the indicated genotypes. Number of TIF-positive, total cells, and independent MEFs per genotype are shown. Fisher exact test was used for statistical analysis, and p-values are indicated. Error bars represent SEM. Bars, 10 µm.

related to increased telomere fragility (Muñoz et al., 2005; Blanco et al., 2007; Martínez et al., 2009; Sfeir et al., 2009). In particular, MTS have been proposed to result from replication fork stalling and increased breakage at telomeres, as they are increased by aphidicolin treatment, which is known to inhibit DNA synthesis and induce DNA breaks at chromosome-fragile sites (Durkin and Glover, 2007). In concordance with this notion, MTS were increased in wild-type MEFs treated with aphidicolin and further increased in *SIRT1*-deficient MEFs (Fig. 6, A, C, and D), suggesting that *SIRT1*-deficient cells are more prone to replication fork stalling and breakage. However, chromosome end-to-end fusions were not increased by *SIRT1* deficiency, indicating that SIRT1 is not essential for telomere capping (Fig. 6 B). Importantly, SIRT1 overexpression in *SIRT1*^{super} MEFs did not increase MTS or any other type of telomere aberration (Fig. 6, A–D), again supporting the notion that increased SIRT1 expression has no deleterious effects on telomere function and integrity. Absence of TIFs and telomere aberrations (fusions and MTS) associated with SIRT1-increased expression is in agreement with normal telomere capping in these cells. Notably, decreased SFE associated with SIRT1 overexpression (Figs. 1 and 3) may reflect longer telomeres in these cells, as not all SFEs (telomeres under the Q-FISH detection level) correspond to TIFs.

SIRT1-mediated deacetylation of telomeric and pericentromeric regions

Telomeric chromatin is composed of TTAGGG repeats bound by shelterin. Mammalian telomeres also contain arrays of nucleosomes enriched in histone heterochromatic marks (Blasco, 2007), and they are associated with long, noncoding telomeric RNAs or TERRA (Azzalin et al., 2007; Schoeftner and Blasco, 2008). Telomeric and subtelomeric chromatin are characterized by a high density of H3K9me3 and H4K20me3 histone trimethylation marks and by HP1 binding (García-Cao et al., 2004;

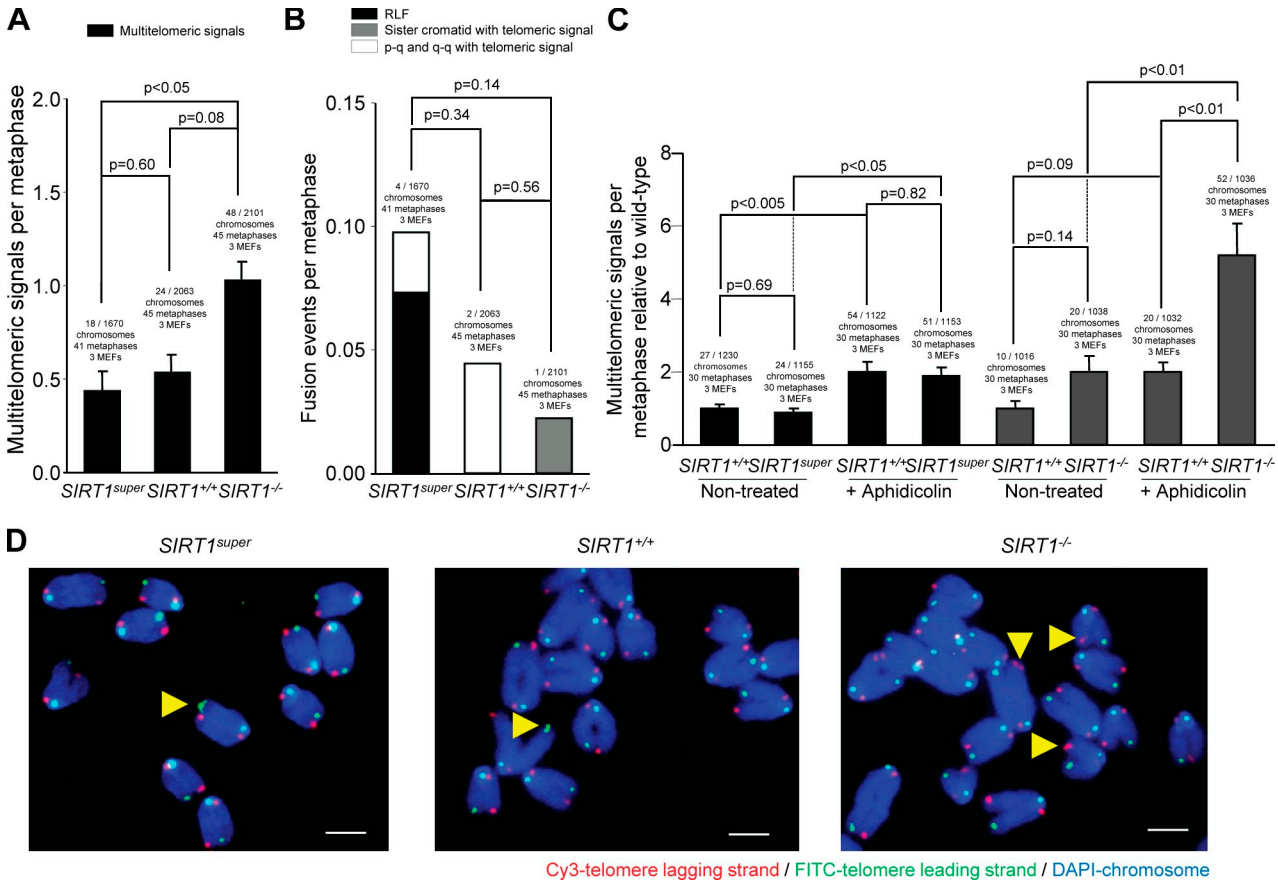

Figure 6. **SIRT1 deficiency leads to increased MTS related to telomere fragility.** (A) Quantification of MTS in primary (passage 2) MEFs of the indicated genotypes. (B) Quantification of end to end fusions in MEFs of the indicated genotypes. (C) Quantification of fold increase in MTS in metaphases of the indicated genotypes with and without treatment with aphidicolin compared with wild-type MEFs. Cells were treated with aphidicolin when indicated. SEM and the number of chromosomes, metaphases, and telomeres used for the analysis are shown for each genotype. The Fisher exact test was used for statistical calculations, and p-values are indicated. (D) Representative images showing increased MTS in *SIRT1*-deficient MEFs are shown. Telomere lagging strand is shown in red, leading strand in green, and DAPI staining in blue. Yellow arrowheads indicate the MTS. Bars, 1 µm.

Gonzalo et al., 2005). In addition, subtelomeric DNA repeats are heavily methylated (Blasco, 2007).

Given that SIRT1 has histone deacetylase activity, we first set to determine the abundance of different histone marks at telomeric and pericentromeric chromatin in *SIRT1*^{super} MEFs and their corresponding wild-type controls by using chromatin immunoprecipitation (ChIP) followed by detection of telomeric repeats (see Materials and methods). Interestingly, we observed a significant reduction in the density of H3K9Ac at telomeres when SIRT1 deacetylase was overexpressed (Fig. 7, A and B). These results are in line with a role of SIRT1 in regulation of acetylation levels at mammalian telomeres. Interestingly, when a similar analysis was performed on pericentromeric chromatin, we also observed decreased H3K9Ac, which almost reached significance, and a significant increase in H4K20me3 trimethylation (Fig. 7, C and D), which is suggestive of induction of a more heterochromatic state. In line with this, when we performed a similar ChIP analysis on *SIRT1*$^{-/-}$ MEFs, we observed that absence of *SIRT1* results in a significant decrease of the heterochromatic marks H3K9me3 and HP1-γ at telomeric repeats (Fig. 7, E and F), a trend that did not reach significance in the case of pericentomeric repeats (Fig. 7, G and H). ChIP values were corrected both by the respective telomere and centromere inputs and by H3 and H4 abundance at these regions (Fig. 7). We did not detect significant changes in the density of the TRF1 shelterin protein at telomeres (Fig. 7, A, B, E, and F). As negative control, TRF1 was not bound to pericentromeric chromatin (Fig. 7, C, D, G, and H). Together, these results suggest that SIRT1 levels negatively modulate histone acetylation at telomeric chromatin, concomitantly increasing heterochromatic marks such as H3K9me3 and H4K20me3.

We next analyzed the impact of both *SIRT1* deficiency and SIRT1-increased expression on global DNA methylation measured as the proportion of methylated CpG at the B1 SINE repeats, and we determined DNA methylation of subtelomeric sequences located at chromosomes 1 and 2 by bisulphite sequencing (see Materials and methods). As shown in Fig. S3 and Fig. S4, we did not find significant differences in DNA methylation levels at these regions between *SIRT1*^{super}, *SIRT1*$^{-/-}$, and their respective wild-type controls.

SIRT1 specifically binds to telomeric repeats in vivo in induced pluripotent stem (iPS) cells

To address whether the effects of SIRT1 on telomere length, telomere heterochromatin, and telomere integrity (fragility and

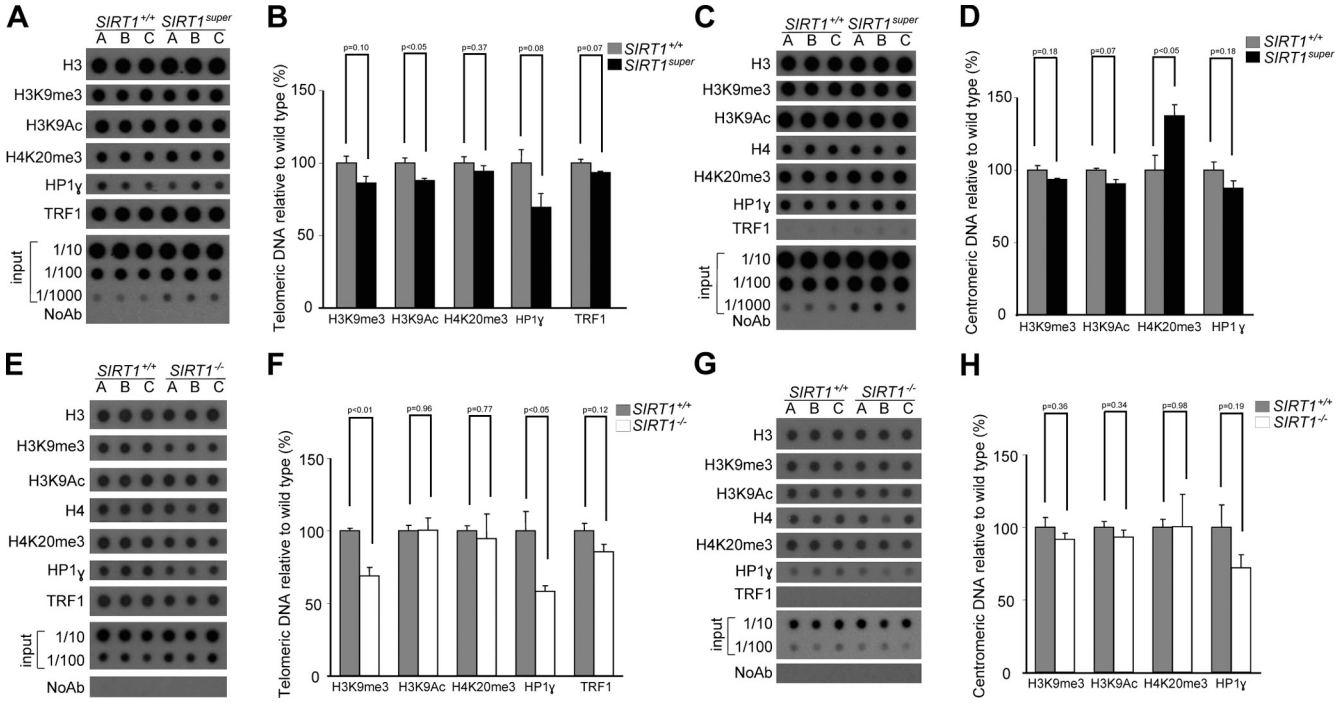

Figure 7. **SIRT1-increased expression decreases histone acetylation at telomeric and centromeric chromatin.** (A, C, E, and G) ChIP was performed with primary (passage 2) MEFs of the indicated genotypes (n = 3) using specific antibodies against H3, H3K9me3, H3K9Ac, H4K20me3, HP1-γ, and TRF1. Immunoprecipitated material was transferred to a nitrocellulose membrane and probed with a 1.6-kb telomeric probe (A and E) or probed with a mouse major satellite probe (C). (B, D, F, and H) Quantification of ChIP values for telomere and centromere repeats as indicated. The amount of immunoprecipitated DNA was normalized for the amount of telomere or centromeric repeats present in the cross-linked chromatin fraction unbound to the preimmune serum (input). n = number of independent MEFs used. Bars represent the mean between replicates, and SEM is shown. A Student's t test was used to calculate statistical significance, and p-values are shown.

recombination) were mediated by binding of SIRT1 to telomeres in vivo, we performed ChIP analysis of telomeric and centromeric repeats with SIRT1 antibodies. We did not detect specific SIRT1 binding to telomeric chromatin in MEFs. To rule out this apparent lack of SIRT1 binding to telomeric repeats as the result of a transient association, we set to perform SIRT1 ChIP analysis in cells with very long telomeres such as those of pluripotent stem cells (Flores et al., 2008; Marion et al., 2009b). Interestingly, stem cells express high levels of SIRT1 compared with differentiated tissues (McBurney et al., 2003; Kuzmichev et al., 2005; Saunders et al., 2010), and SIRT1 has been shown to regulate neural and glial specification of neural precursors (Prozorovski et al., 2008), differentiation of skeletal myoblasts (Fulco et al., 2008), and to inhibit spermatogenesis (Coussens et al., 2008). To this end, we produced iPS from *SIRT1*$^{+/+}$ and *SIRT1*$^{-/-}$ MEFs and evaluated SIRT1 binding to telomere repeats in vivo. As shown by ChIP analysis, SIRT1 specifically binds to telomeric repeats but not to pericentric major satellite regions in iPS cells (Fig. 8, A and B). These results suggest that SIRT1 effects on telomere function and in length regulation may be mediated by binding of SIRT1 to telomeric repeats.

Discussion

The Sir2 family of nutrient-responsive NAD$^+$-dependent deacetylases has emerged as key regulator of lifespan in yeast and other organisms (Haigis and Guarente, 2006). CR studies have shown that SIRT1, the closest mammalian homologue of yeast Sir2, also plays an important role in longevity and resistance to age-associated diseases in higher organisms by increasing health span (Chen et al., 2005; Bordone et al., 2007; Boily et al., 2008; Campisi and Yaswen, 2009; Cantó and Auwerx, 2009; Cohen et al., 2009; Saunders and Verdin, 2009; Herranz et al., 2010). However, the molecular mechanisms by which SIRT1 impacts on CR, lifespan, and health span are still largely unknown (Wood et al., 2004).

Telomere shortening is associated with organismal aging and increased telomeric damage, proposed to be causative of aging-associated pathologies in humans (Blasco et al., 1997; Flores et al., 2005; Ornish et al., 2008; Martínez et al., 2009). Generation of the first knockout mice for the telomerase RNA component (Blasco et al., 1997) showed a conserved role for telomerase as the main activity responsible for maintaining telomere length in mammals and uncovered its importance in tissue renewal and lifespan and showed that short telomeres could cause multiple defects associated with decreased adult stem cell functionality. Remarkably, telomerase-deficient mice from the first generation already show a decreased median and maximum life span, indicating that telomere length and telomerase are rate limiting for mouse longevity in spite of mice born with very long telomeres (García-Cao et al., 2004). This is in line with recent findings showing that mouse telomeres suffer a dramatic shortening when comparing old (2-yr old) with young individuals (2-mo old; Flores et al., 2008). Furthermore, decreasing the rate of telomere erosion by forcing telomerase expression in adult tissues significantly delays aging and extends

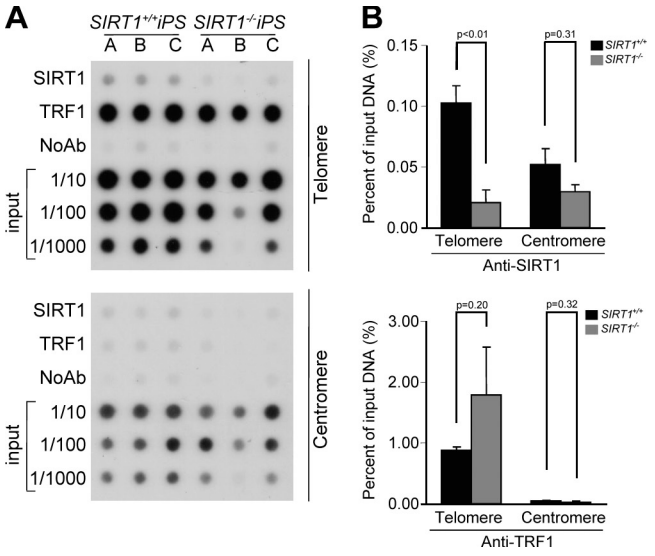

Figure 8. **SIRT1 protein interacts with telomeric repeats in vivo in iPS cells.** (A) ChIP was performed with iPS cells of the indicated genotype (n = 3) using antibodies against SIRT1 and TRF1. Immunoprecipitated material was transferred to a nitrocellulose membrane and probed with a 1.6-kb telomeric probe (top) and a mouse major satellite (bottom). (B) Quantification of ChIP values for telomere and centromere repeats as indicated. The amount of immunoprecipitated DNA was normalized for the amount of telomere or centromeric repeats present in the cross-linked chromatin fraction unbound to the preimmune serum (input). n = number of independent MEFs used. Bars represent the mean between replicates, and SEM is shown. A Student's t test was used to calculate statistical significance, and p-values are shown.

the mean lifespan of cancer-resistant mice by 40% (Tomás-Loba et al., 2008).

In this study, we set out to address whether SIRT1 may have an impact on telomere length maintenance by studying both loss of function (*SIRT1*$^{-/-}$ mice) and gain of function mouse models for SIRT1 (*SIRT1*^{super} mice). The latter mouse model is particularly interesting for aging studies, as we recently showed that *SIRT1*^{super} mice have an increased health span and are protected from metabolic syndrome and liver cancer associated with metabolic syndrome (Pfluger et al., 2008; Herranz et al., 2010). Furthermore, several SIRT1 direct and indirect activators, including resveratrol, have been recently described to have beneficial effects on several age-associated diseases (Baur et al., 2006; Lagouge et al., 2006; Milne et al., 2007; Feige et al., 2008; Pearson et al., 2008; Yamazaki et al., 2009).

In this study, we find that overexpression of SIRT1 in mice decreases the rate of telomere erosion associated with cell division and tissue aging (i.e., liver and kidney), whereas SIRT1 abrogation results in an increased telomere erosion. The beneficial effects of increased SIRT1 activity on telomere length maintenance occur without any detrimental effects on telomere integrity or telomere capping. Furthermore, we show that improved maintenance of telomeres in *SIRT1*^{super} cells is dependent on an active telomerase complex, suggesting that SIRT1-increased expression impacts the telomerase pathway. Interestingly, it has been previously described that silencing of SIRT1 by RNAi results in an increase of telomerase expression in HeLa cells (Narala et al., 2008). Our findings suggest that the increased health span of *SIRT1*^{super} mice may be due, at least in part, to a better maintenance of telomere length with increasing age (Pfluger et al., 2008; Herranz et al., 2010). Interestingly, both mean and maximum longevity are not increased in *SIRT1*^{super} mice in spite of increased health span (Herranz et al., 2010) and longer telomeres (this study), which goes in line with our recent observations that improved telomere maintenance increases longevity only when in highly cancer-resistant backgrounds (Tomás-Loba et al., 2008). Finally, these findings also open the interesting possibility that SIRT1-dependent effects of CR, or the beneficial effects of SIRT1 activators, could be partially mediated by SIRT1-positive effects on telomere length maintenance, although this remains to be addressed.

In addition, *SIRT1*^{super} cells showed augmented frequencies of sister chromatid homologous recombination events at telomeres, centromeres, and chromosome arms, indicating that SIRT1-increased expression significantly impacts homologous recombination. Interestingly, these results also suggest that increased SIRT1 expression may positively impact DNA repair efficiency, thereby also contributing to increased tissue fitness and health span. In support of this, SIRT1 has been implicated in protection from DNA damage–induced cell death and carcinogenesis (Oberdoerffer et al., 2008; Wang et al., 2008; Herranz et al., 2010). Finally, SIRT1 is likely to influence homologous recombination through deacetylation of Nbs1 and WRN helicase, two important players in DNA repair by homologous recombination (Yuan et al., 2007; Uhl et al., 2010).

In contrast with the effects of SIRT1 overexpression on telomere length maintenance and improved homologous recombination, we found that SIRT1 deficiency had a negative impact both on telomere length maintenance and telomere integrity, which is in agreement with recent data (El Ramy et al., 2009). In particular, *SIRT1*$^{-/-}$ MEF showed an increase in chromosomes with MTS, which are further increased by aphidicolin treatment, indicative of increased telomere fragility and breakage. Accordingly, cells lacking SIRT1 showed a higher level of telomere damage (TIFs). Together, these findings suggest a role of SIRT1 on preventing telomere damage, which could again be mediated by some of its known deacetylation targets, including Nbs1 and WRN. Additionally, SIRT1-altered expression resulted in changes in the heterochromatic status of telomeres, which go in line with a model where SIRT1 levels negatively modulate histone acetylation at telomeric chromatin, concomitantly increasing heterochromatic marks such as H3K9me3 and H4K20me3. Previous studies have shown that SIRT1 can deacetylate H3K9Ac and H4K16Ac (Vaquero et al., 2004; Vaquero et al., 2007), H3K56Ac (Chen et al., 2008; Das et al., 2009), and H3K26Ac (Oberdoerffer et al., 2008) and as a consequence of decreased acetylation, can lead to higher abundance of heterochromatic marks like H2K9me3 and H4K20me1 (Vaquero et al., 2004). A SIRT1-dependent increase in H4K20me3 has not been previously reported. However, SIRT1 can specifically target the histone methyltransferase suppressor of variegation 3-9 homologue (Suv39h1), leading to increased H2K9me3 (Vaquero et al., 2007), and therefore, H2K9me3 recruits HP1, which is necessary to assemble H4K20me3 at pericentric chromatin (Schotta et al., 2004). Importantly, we show in this study that SIRT1 can interact in vivo with telomeric repeats in the

context of iPS cells, arguing that SIRT1 roles in regulation of telomere length, integrity, and recombination and telomere heterochromatin could be explained at least in part by a direct SIRT1 binding to telomeres in vivo.

In summary, the findings described in this study demonstrate that increased expression of SIRT1, the closest mammalian orthologue of yeast Sir2, improves telomere length maintenance in vivo and significantly increases recombination frequencies at telomeres, centromeres, and chromosome arms. These effects of increased SIRT1 expression are potentially beneficial to preserve genome integrity and stability and open new avenues to understand the known effects of increased SIRT1 expression on health span and protection from some age-associated diseases.

Materials and methods

Mice

SIRT1^{super} (C57BL/6 background) and *SIRT1*$^{-/-}$ (mixed 129/Sv and C57BL/6 background) mice were provided by M. Serrano (Spanish National Cancer Centre, Madrid, Spain; Pfluger et al., 2008) and F. Alt (Harvard University, Cambridge, MA), respectively (Cheng et al., 2003). To generate *SIRT1*^{super} *Terc*$^{+/+}$, *SIRT1*$^{+/+}$ *Terc*$^{+/+}$, *SIRT1*$^{+/+}$ *Terc*$^{+/+}$, and *SIRT1*$^{+/+}$ *Terc*$^{-/-}$ mice, *SIRT1*^{super} mice were crossed with *Terc*$^{-/-}$ (C57BL/6 background) animals (Blasco et al., 1997), and the resulting double-heterozygous breeding pairs were used to generate G1 (first generation) of single *Terc*$^{-/-}$ *SIRT1*^{super} and *SIRT*$^{+/+}$ mice. Mice were housed in a Specific Pathogen Free facility and treated according to the Federations of European Laboratory and Animal Science Association. All animals were maintained in a normal maintenance diet (2018; Harlan Laboratories).

Cell culture

Primary MEFs (passage 2) were obtained from *SIRT1*$^{+/+}$, *SIRT1*$^{-/-}$, *SIRT1*^{super}, *SIRT1*^{super} *Terc*$^{+/+}$, *SIRT1*$^{+/+}$ *Terc*$^{+/+}$, *SIRT1*$^{+/+}$ *Terc*$^{+/+}$, and *SIRT1*$^{+/+}$ *Terc*$^{-/-}$ embryos as described previously (Blasco et al., 1997). To generate iPS cells, MEFs from the indicated genotypes were reprogrammed as described previously (Marión et al., 2009a,b). *SIRT1*$^{+/+}$ and *SIRT1*$^{-/-}$ MEFs were transfected with pHA-SIRT1 (#10962; Addgene) or pCruz-HA (sc-5045; Santa Cruz Biotechnology, Inc.) plasmids using the Neon Transfection System (Invitrogen) according to the manufacturer's conditions, and cells were harvested 4 d after transfection.

Telomerase assay

Telomerase activity was measured with a modified TRAP as previously described (Blasco et al., 1997). Whole cell extracts were incubated with $(UUAGGG)_3$ or $(CCCUAA)_3$ RNA oligonucleotides for 5 min on ice and for 5 min at room temperature before beginning the telomerase extension reaction. To degrade spiked RNA oligonucleotides before PCR amplification, samples were treated with 10 pg RNase A (QIAGEN) at room temperature for 20 min.

Immunoblotting

Cells were harvested by trypsinization, washed once with PBS, lysed with cold RIPA, resuspended in SDS-PAGE loading buffer, and sonicated. Equal amounts of protein (50–100 mg) were analyzed by gel electrophoresis followed by Western blotting. The following antibodies were used for immunoblotting: rabbit anti-SIRT1 (ab12913; Abcam), mouse anti-HA (sc-7392; Santa Cruz Biotechnology, Inc.), and anti–α-tubulin (T6557; Sigma-Aldrich) as a loading control. Antibody binding was detected after incubation with a secondary antibody coupled to horseradish peroxidase using enhanced chemiluminescence.

Immunofluorescence

MEFs growing in coverslips were permeabilized by incubation in PBS with 0.5% BSA and 0.1% Triton X-100 for 15 min. After permeabilization, slides were blocked in 2% BSA for 1 h and incubated with primary antibody. Permeabilized sections were incubated with rabbit anti-TRF1 (1:200) prepared as described previously (Muñoz et al., 2005), mouse monoclonal anti-phospho–histone H2AX antibody (1:500; Millipore), and secondary antibodies Cy3-conjugated goat anti–rabbit (1:400) and Alexa Fluor 555 donkey anti–mouse (1:300; Jackson ImmunoResearch Laboratories, Inc.). Slides were washed in PBS with 0.1% Triton X-100 and mounted in Vectashield with DAPI (Vector Laboratories). Confocal microscopy was performed at room temperature with a laser-scanning microscope (TCS SP5; Leica) using a Plan Apo 63× 1.40 NA oil immersion objective (HCX; Leica). The pictures show the maximal projection of z stacks generated using advanced fluorescence software (LAS; Leica).

Telomere and fluorescence analyses on liver and kidney sections

Q-FISH was performed directly on liver and kidney sections as previously described (Zijlmans et al., 1997; Muñoz et al., 2005). Confocal microscopy was performed at room temperature with a laser-scanning microscope (TCS SP5) using a Plan Apo 63× 1.40 NA oil immersion objective (HCX). The pictures show the maximal projection of z stacks generated using advanced fluorescence software (LAS). Images were analyzed with Definiens XD software package. The DAPI image was use to define the nuclear area, and the fluorescent PNA telomeric probe screen was used to detect single telomeric signal inside of each nuclei.

Telomere length and cytogenetic analysis using telomere Q-FISH on metaphases

We prepared metaphases and performed Q-FISH hybridization as previously described (Samper et al., 2000; Gonzalo et al., 2006). To correct for lamp intensity and alignment, images from fluorescent beads (Invitrogen) were analyzed in parallel using the TFL-Telo program (provided by P. Lansdorp, British Columbia Cancer Research Centre, Vancouver, British Columbia, Canada). Telomere fluorescence values were extrapolated from the telomere fluorescence of lymphoma cell lines LY-R (R cells) and LY-S (S cells) with known telomere lengths of 80 kb and 10 kb, respectively. We captured the images at room temperature using a charge-coupled device camera (FK7512; COHU) on a fluorescence microscope (DMRB; Leica) with a Plan Apo 100× 1.40 NA oil immersion objective (HCX; Leica) using Q-FISH software (Leica) in a linear acquisition mode to prevent the saturation of fluorescence intensity. TFL-Telo software (Zijlmans et al., 1997) was used to quantify the fluorescence intensity of telomeres from at least 10–15 metaphases for each data point. When indicated, primary MEFs were treated with 0.5 µM aphidicolin for 24 h. For analysis of chromosomal aberrations, metaphases were analyzed by superimposing the telomere image on the DAPI image using the TFL-Telo software.

TRF analysis

Cells were included in agarose plugs, and TRF analysis was performed as described previously (Blasco et al., 1997). Mean telomere length was calculated by densitometric analysis using ImageJ (National Institutes of Health). After building 2D representation of signal intensity of each lane, mean telomere length was defined as the intersection point of intersection of the x axis and a line that divided the area below the curve in equal parts.

B1-SINE Cobra analysis for global DNA methylation

Global DNA methylation levels were determined using the B1-SINE Cobra method as previously described (Benetti et al., 2007a,b). Estimation of the fraction of methylated B1 elements for each genotype was performed using the following formula: ([molarity of 45-bp band]/2)/([molarity of 45-bp band] + [molarity of 100-bp band]).

Analysis of genomic subtelomeric DNA methylation

DNA methylation of subtelomeric genomic regions of chromosomes 1 and 2 (q-arms) was performed by PCR analysis after bisulfite modification as described previously (Benetti et al., 2007a,b). To examine the methylation status of subtelomeric CpG islands, 17–55 colonies were automatically sequenced for each cell line. Bisulfite genomic sequencing primers used against subtelomeric regions in chromosomes 1 and 2 were 5′-CACCTCTAACCACTTAAACCTAACAA-3′ and 5′-GGGAGTGGAAGGAATTAGTAGGTT-3′, which flank positions 197,042,227–197,042,569 of chromosome 1 in the mouse NCBI36 genome assembly, and 5′-TTACCAATACCACCATTCCTCCA-3′ and 5′-GAGAGTAGTTAATTAGATGAGGAATA-3′, which flank positions 181,837,807–181,838,281 at chromosome 2 in the mouse NCBI36 genome assembly. Results were analyzed for DNA methylation analysis using BiQ Analyzer software (Applied Biosystems).

ChIP assay

ChIP assays were performed as previously described (García-Cao et al., 2004). In brief, after cross-linking and sonication, chromatin from 4×10^6 cells were used per each immunoprecipitation with Protein A/G Plus agarose beads (sc-2003; Santa Cruz Biotechnology, Inc.) and the following antibodies: 6 µg anti–histone H3 (ab1791; Abcam), 6 µg anti–histone H4

(ab10158; Abcam), 6 µg anti-H3K9me3 (#07-442; Millipore), 6 µg anti-H4K20me3 (#07-749; Millipore), 6 µg anti-SIRT1 (ab12193; Abcam), 8 µl rabbit polyclonal antibody to TRF1 (raised in our laboratory against full-length mouse TRF1 protein), and 10 µl monoclonal anti–γ-HP1 (#05-690; Millipore) or preimmune serum. The immunoprecipitated DNA was transferred to a Hybond N+ membrane using a dot blot apparatus. The membrane was then hybridized with either a telomeric probe containing TTAGGG repeats or a probe recognizing major satellite sequences, which is characteristic of pericentric heterochromatin. Quantification of the signal was performed with ImageQuant software (Molecular Dynamics). The amount of telomeric and pericentric DNA after ChIP was normalized for the total telomeric or centromeric DNA signal, respectively, for each genotype and for the H3 and H4 abundance at these regions, thus correcting for differences in the number of telomere repeats or in nucleosome spacing.

CO-FISH

Cells were subcultured in the presence of BrdU (Sigma-Aldrich) at a final concentration of 10^{-5} M and allowed to replicate their DNA once at 37°C. Colcemid was added in a concentration of 0.2 µg/ml for the last 4 h. Cells were recovered, and metaphases were prepared as previously described (Samper et al., 2000). CO-FISH was performed as previously described (Gonzalo et al., 2006) using first a telomeric $(CCCTAA)_7$ PNA probe labeled with Cy3, a second telomeric $(TTAGGG)_7$ PNA probe labeled with fluorescein, or a minor satellite PNA probe labeled with Cy3 (Cy3-oo-TTCCAACGAATGTGTTTT), which hybridizes with the lagging DNA strand, followed by a second hybridization with a minor satellite PNA probe labeled with FITC (Flu-oo-AAAACACATTCGTTGGAA), which hybridizes with the leading DNA strand (Applied Biosystems). Metaphase spreads were captured on a fluorescence microscope (DMRB; Leica).

Differential staining technique for SCE determinations

Genomic SCEs were visualized using an adapted fluorescence plus Giemsa protocol (Perry and Wolff, 1974). MEFs were grown at 37°C for two rounds of DNA replication in the presence of 3 µg/ul BrdU. Colcemid was added in a concentration of 0.2 µg/ml for the last 4 h. Cells were then recovered, and metaphases were prepared as described previously (Samper et al., 2000). Metaphase spreads on slides were immersed in 5 µg/ml Hoechst 333258 solution (Invitrogen) and washed with abundant water. The slides were exposed to UV light for 15 min in the presence of 2× SSC, washed with water, stained with Giemsa solution (Merck) for 2 min, and washed with water. Images were captured using a brightfield microscope (AX70; Olympus) using a Plan Apo 100× 1.4 NA oil immersion objective. Images were captured using a color camera (DP70; Olympus) and Image-Pro Plus high-end image acquisition and analysis software (Media Cybernetics). All of the image capture was performed at room temperature. Metaphases were analyzed for harlequin staining. Each color switch was scored as one SCE.

Statistical analysis

Student's *t* test was performed using Excel (97; Microsoft) or Prism software (version 5; GraphPad Software, Inc.). Fisher exact test was performed using SPSS version 15.

Online supplemental material

Fig. S1 shows TRF analysis of primary MEFs (*SIRT1*^{super}, *SIRT1*$^{+/+}$;*SIRT1*$^{+/+}$, and *SIRT1*$^{-/-}$) and quantification of their mean telomere length per genotype. Fig. S2 shows Western immunoblotting against SIRT1 and tubulin in primary MEFs of *SIRT1*$^{+/+}$ and *SIRT1*$^{-/-}$ transfected with SIRT1 coding (pHA-SIRT1) and control plasmid. Fig. S3 shows global DNA methylation measured as methylations of B1-SINE repeats in primary MEFs (*SIRT1*^{super}, *SIRT1*$^{+/+}$;*SIRT1*$^{+/+}$, and *SIRT1*$^{-/-}$). Fig. S4 shows subtelomeric DNA methylation of chromosomes 1 and 2 in MEFs (*SIRT1*^{super}, *SIRT1*$^{+/+}$; *SIRT1*$^{+/+}$, and *SIRT1*$^{-/-}$). Fig. S5 shows survival curves of *SIRT1*^{super} x *Terc*$^{+/+}$, *SIRT1*^{super} x *Terc*$^{-/-}$, *SIRT1*$^{+/+}$ x *Terc*$^{+/+}$, and *SIRT1*$^{+/+}$ x *Terc*$^{-/-}$ mice. Online supplemental material is available at http://www.jcb.org/cgi/content/full/jcb.201005160/DC1.

J.A. Palacios is funded by a Juan de la Cierva contract from the Spanish Ministry of Innovation and Science. M.A. Blasco's laboratory is funded by the Spanish Ministry of Innovation and Science, the European Union (FP7-Genica), the European Research Council (ERC Advance Grants), the Spanish Association Against Cancer (AECC), and the Körber European Science Award (to M.A. Blasco).

Submitted: 31 May 2010
Accepted: 29 November 2010

References

Abdelmohsen, K., R. Pullmann Jr., A. Lal, H.H. Kim, S. Galban, X. Yang, J.D. Blethrow, M. Walker, J. Shubert, D.A. Gillespie, et al. 2007. Phosphorylation of HuR by Chk2 regulates SIRT1 expression. *Mol. Cell.* 25:543–557. doi:10.1016/j.molcel.2007.01.011

Azzalin, C.M., P. Reichenbach, L. Khoriauli, E. Giulotto, and J. Lingner. 2007. Telomeric repeat containing RNA and RNA surveillance factors at mammalian chromosome ends. *Science.* 318:798–801. doi:10.1126/science.1147182

Bailey, S.M., E.H. Goodwin, J. Meyne, and M.N. Cornforth. 1996. CO-FISH reveals inversions associated with isochromosome formation. *Mutagenesis.* 11:139–144. doi:10.1093/mutage/11.2.139

Bailey, S.M., M.A. Brenneman, and E.H. Goodwin. 2004. Frequent recombination in telomeric DNA may extend the proliferative life of telomerase-negative cells. *Nucleic Acids Res.* 32:3743–3751. doi:10.1093/nar/gkh691

Baur, J.A., K.J. Pearson, N.L. Price, H.A. Jamieson, C. Lerin, A. Kalra, V.V. Prabhu, J.S. Allard, G. Lopez-Lluch, K. Lewis, et al. 2006. Resveratrol improves health and survival of mice on a high-calorie diet. *Nature.* 444:337–342. doi:10.1038/nature05354

Bedalov, A., T. Gatbonton, W.P. Irvine, D.E. Gottschling, and J.A. Simon. 2001. Identification of a small molecule inhibitor of Sir2p. *Proc. Natl. Acad. Sci. USA.* 98:15113–15118. doi:10.1073/pnas.261574398

Benetti, R., M. García-Cao, and M.A. Blasco. 2007a. Telomere length regulates the epigenetic status of mammalian telomeres and subtelomeres. *Nat. Genet.* 39:243–250. doi:10.1038/ng1952

Benetti, R., S. Gonzalo, I. Jaco, G. Schotta, P. Klatt, T. Jenuwein, and M.A. Blasco. 2007b. Suv4-20h deficiency results in telomere elongation and derepression of telomere recombination. *J. Cell Biol.* 178:925–936. doi:10.1083/jcb.200703081

Blagoev, K.B., and E.H. Goodwin. 2008. Telomere exchange and asymmetric segregation of chromosomes can account for the unlimited proliferative potential of ALT cell populations. *DNA Repair (Amst.).* 7:199–204. doi:10.1016/j.dnarep.2007.09.012

Blanco, R., P. Muñoz, J.M. Flores, P. Klatt, and M.A. Blasco. 2007. Telomerase abrogation dramatically accelerates TRF2-induced epithelial carcinogenesis. *Genes Dev.* 21:206–220. doi:10.1101/gad.406207

Blasco, M.A. 2005. Telomeres and human disease: ageing, cancer and beyond. *Nat. Rev. Genet.* 6:611–622. doi:10.1038/nrg1656

Blasco, M.A. 2007. The epigenetic regulation of mammalian telomeres. *Nat. Rev. Genet.* 8:299–309. doi:10.1038/nrg2047

Blasco, M.A., H.W. Lee, M.P. Hande, E. Samper, P.M. Lansdorp, R.A. DePinho, and C.W. Greider. 1997. Telomere shortening and tumor formation by mouse cells lacking telomerase RNA. *Cell.* 91:25–34. doi:10.1016/S0092-8674(01)80006-4

Boily, G., E.L. Seifert, L. Bevilacqua, X.H. He, G. Sabourin, C. Estey, C. Moffat, S. Crawford, S. Saliba, K. Jardine, J. Xuan, M. Evans, M.E. Harper, and M.W. McBurney. 2008. SirT1 regulates energy metabolism and response to caloric restriction in mice. *PLoS One*. 3:e1759.

Bordone, L., D. Cohen, A. Robinson, M.C. Motta, E. van Veen, A. Czopik, A.D. Steele, H. Crowe, S. Marmor, J. Luo, et al. 2007. SIRT1 transgenic mice show phenotypes resembling calorie restriction. *Aging Cell.* 6:759–767. doi:10.1111/j.1474-9726.2007.00335.x

Brachmann, C.B., J.M. Sherman, S.E. Devine, E.E. Cameron, L. Pillus, and J.D. Boeke. 1995. The SIR2 gene family, conserved from bacteria to humans, functions in silencing, cell cycle progression, and chromosome stability. *Genes Dev.* 9:2888–2902. doi:10.1101/gad.9.23.2888

Broccoli, D., A. Smogorzewska, L. Chong, and T. de Lange. 1997. Human telomeres contain two distinct Myb-related proteins, TRF1 and TRF2. *Nat. Genet.* 17:231–235. doi:10.1038/ng1097-231

Brooks, C.L., and W. Gu. 2009. How does SIRT1 affect metabolism, senescence and cancer? *Nat. Rev. Cancer.* 9:123–128. doi:10.1038/nrc2562

Bühler, M., and S.M. Gasser. 2009. Silent chromatin at the middle and ends: lessons from yeasts. *EMBO J.* 28:2149–2161. doi:10.1038/emboj.2009.185

Campisi, J., and P. Yaswen. 2009. Aging and cancer cell biology, 2009. *Aging Cell.* 8:221–225. doi:10.1111/j.1474-9726.2009.00475.x

Canela, A., E. Vera, P. Klatt, and M.A. Blasco. 2007. High-throughput telomere length quantification by FISH and its application to human population studies. *Proc. Natl. Acad. Sci. USA.* 104:5300–5305. doi:10.1073/pnas.0609367104

Cantó, C., and J. Auwerx. 2009. Caloric restriction, SIRT1 and longevity. *Trends Endocrinol. Metab.* 20:325–331. doi:10.1016/j.tem.2009.03.008

Cawthon, R.M., K.R. Smith, E. O'Brien, A. Sivatchenko, and R.A. Kerber. 2003. Association between telomere length in blood and mortality in people aged 60 years or older. *Lancet.* 361:393–395. doi:10.1016/S0140-6736(03)12384-7

Chan, S.W., and E.H. Blackburn. 2002. New ways not to make ends meet: telomerase, DNA damage proteins and heterochromatin. *Oncogene.* 21:553–563. doi:10.1038/sj.onc.1205082

Chan, S.R., and E.H. Blackburn. 2004. Telomeres and telomerase. *Philos. Trans. R. Soc. Lond. B Biol. Sci.* 359:109–121. doi:10.1098/rstb.2003.1370

Chen, D., A.D. Steele, S. Lindquist, and L. Guarente. 2005. Increase in activity during calorie restriction requires Sirt1. *Science.* 310:1641. doi:10.1126/science.1118357

Chen, C.C., J.J. Carson, J. Feser, B. Tamburini, S. Zabaronick, J. Linger, and J.K. Tyler. 2008. Acetylated lysine 56 on histone H3 drives chromatin assembly after repair and signals for the completion of repair. *Cell.* 134:231–243. doi:10.1016/j.cell.2008.06.035

Cheng, H.L., R. Mostoslavsky, S. Saito, J.P. Manis, Y. Gu, P. Patel, R. Bronson, E. Appella, F.W. Alt, and K.F. Chua. 2003. Developmental defects and p53 hyperacetylation in Sir2 homolog (SIRT1)-deficient mice. *Proc. Natl. Acad. Sci. USA.* 100:10794–10799. doi:10.1073/pnas.1934713100

Cohen, D.E., A.M. Supinski, M.S. Bonkowski, G. Donmez, and L.P. Guarente. 2009. Neuronal SIRT1 regulates endocrine and behavioral responses to calorie restriction. *Genes Dev.* 23:2812–2817. doi:10.1101/gad.1839209

Collins, K., and J.R. Mitchell. 2002. Telomerase in the human organism. *Oncogene.* 21:564–579. doi:10.1038/sj.onc.1205083

Coussens, M., J.G. Maresh, R. Yanagimachi, G. Maeda, and R. Allsopp. 2008. Sirt1 deficiency attenuates spermatogenesis and germ cell function. *PLoS One.* 3:e1571. doi:10.1371/journal.pone.0001571

d'Adda di Fagagna, F., P.M. Reaper, L. Clay-Farrace, H. Fiegler, P. Carr, T. Von Zglinicki, G. Saretzki, N.P. Carter, and S.P. Jackson. 2003. A DNA damage checkpoint response in telomere-initiated senescence. *Nature.* 426:194–198. doi:10.1038/nature02118

Das, C., M.S. Lucia, K.C. Hansen, and J.K. Tyler. 2009. CBP/p300-mediated acetylation of histone H3 on lysine 56. *Nature.* 459:113–117. doi:10.1038/nature07861

de Lange, T. 2005. Shelterin: the protein complex that shapes and safeguards human telomeres. *Genes Dev.* 19:2100–2110. doi:10.1101/gad.1346005

de Lange, T. 2009. How telomeres solve the end-protection problem. *Science.* 326:948–952. doi:10.1126/science.1170633

Dunham, M.A., A.A. Neumann, C.L. Fasching, and R.R. Reddel. 2000. Telomere maintenance by recombination in human cells. *Nat. Genet.* 26:447–450. doi:10.1038/82586

Durkin, S.G., and T.W. Glover. 2007. Chromosome fragile sites. *Annu. Rev. Genet.* 41:169–192. doi:10.1146/annurev.genet.41.042007.165900

El Ramy, R., N. Magroun, N. Messadecq, L.R. Gauthier, F.D. Boussin, U. Kolthur-Seetharam, V. Schreiber, M.W. McBurney, P. Sassone-Corsi, and F. Dantzer. 2009. Functional interplay between Parp-1 and SirT1 in genome integrity and chromatin-based processes. *Cell. Mol. Life Sci.* 66:3219–3234. doi:10.1007/s00018-009-0105-4

Epel, E.S., E.H. Blackburn, J. Lin, F.S. Dhabhar, N.E. Adler, J.D. Morrow, and R.M. Cawthon. 2004. Accelerated telomere shortening in response to life stress. *Proc. Natl. Acad. Sci. USA.* 101:17312–17315. doi:10.1073/pnas.0407162101

Feige, J.N., M. Lagouge, C. Canto, A. Strehle, S.M. Houten, J.C. Milne, P.D. Lambert, C. Mataki, P.J. Elliott, and J. Auwerx. 2008. Specific SIRT1 activation mimics low energy levels and protects against diet-induced metabolic disorders by enhancing fat oxidation. *Cell Metab.* 8:347–358. doi:10.1016/j.cmet.2008.08.017

Flores, I., M.L. Cayuela, and M.A. Blasco. 2005. Effects of telomerase and telomere length on epidermal stem cell behavior. *Science.* 309:1253–1256. doi:10.1126/science.1115025

Flores, I., A. Canela, E. Vera, A. Tejera, G. Cotsarelis, and M.A. Blasco. 2008. The longest telomeres: a general signature of adult stem cell compartments. *Genes Dev.* 22:654–667. doi:10.1101/gad.451008

Frye, R.A. 1999. Characterization of five human cDNAs with homology to the yeast SIR2 gene: Sir2-like proteins (sirtuins) metabolize NAD and may have protein ADP-ribosyltransferase activity. *Biochem. Biophys. Res. Commun.* 260:273–279. doi:10.1006/bbrc.1999.0897

Fulco, M., Y. Cen, P. Zhao, E.P. Hoffman, M.W. McBurney, A.A. Sauve, and V. Sartorelli. 2008. Glucose restriction inhibits skeletal myoblast differentiation by activating SIRT1 through AMPK-mediated regulation of Nampt. *Dev. Cell.* 14:661–673. doi:10.1016/j.devcel.2008.02.004

García-Cao, M., R. O'Sullivan, A.H. Peters, T. Jenuwein, and M.A. Blasco. 2004. Epigenetic regulation of telomere length in mammalian cells by the Suv39h1 and Suv39h2 histone methyltransferases. *Nat. Genet.* 36:94–99. doi:10.1038/ng1278

Gonzalo, S., M. García-Cao, M.F. Fraga, G. Schotta, A.H. Peters, S.E. Cotter, R. Eguía, D.C. Dean, M. Esteller, T. Jenuwein, and M.A. Blasco. 2005. Role of the RB1 family in stabilizing histone methylation at constitutive heterochromatin. *Nat. Cell Biol.* 7:420–428. doi:10.1038/ncb1235

Gonzalo, S., I. Jaco, M.F. Fraga, T. Chen, E. Li, M. Esteller, and M.A. Blasco. 2006. DNA methyltransferases control telomere length and telomere recombination in mammalian cells. *Nat. Cell Biol.* 8:416–424. doi:10.1038/ncb1386

Greider, C.W., and E.H. Blackburn. 1985. Identification of a specific telomere terminal transferase activity in *Tetrahymena* extracts. *Cell.* 43:405–413. doi:10.1016/0092-8674(85)90170-9

Haigis, M.C., and L.P. Guarente. 2006. Mammalian sirtuins—emerging roles in physiology, aging, and calorie restriction. *Genes Dev.* 20:2913–2921. doi:10.1101/gad.1467506

Harley, C.B., A.B. Futcher, and C.W. Greider. 1990. Telomeres shorten during ageing of human fibroblasts. *Nature.* 345:458–460. doi:10.1038/345458a0

Herranz, D., M. Muñoz-Martin, M. Cañamero, F. Mulero, B. Martinez-Pastor, O. Fernandez-Capetillo, and M. Serrano. 2010. Sirt1 improves healthy ageing and protects from metabolic syndrome-associated cancer syndrome. *Nat. Commun.* 1:1–8.

Jaco, I., A. Canela, E. Vera, and M.A. Blasco. 2008. Centromere mitotic recombination in mammalian cells. *J. Cell Biol.* 181:885–892. doi:10.1083/jcb.200803042

Jiang, W.Q., Z.H. Zhong, J.D. Henson, A.A. Neumann, A.C. Chang, and R.R. Reddel. 2005. Suppression of alternative lengthening of telomeres by Sp100-mediated sequestration of the MRE11/RAD50/NBS1 complex. *Mol. Cell. Biol.* 25:2708–2721. doi:10.1128/MCB.25.7.2708-2721.2005

Kahyo, T., R. Mostoslavsky, M. Goto, and M. Setou. 2008. Sirtuin-mediated deacetylation pathway stabilizes Werner syndrome protein. *FEBS Lett.* 582:2479–2483. doi:10.1016/j.febslet.2008.06.031

Kastan, M.B., and D.S. Lim. 2000. The many substrates and functions of ATM. *Nat. Rev. Mol. Cell Biol.* 1:179–186. doi:10.1038/35043058

Kim, E.J., and S.J. Um. 2008. SIRT1: roles in aging and cancer. *BMB Rep.* 41:751–756.

Klar, A.J., S. Fogel, and K. Macleod. 1979. MAR1-a regulator of the HMa and HMalpha loci in *Saccharomyces cerevisiae*. *Genetics.* 93:37–50.

Konig, P., R. Giraldo, L. Chapman, and D. Rhodes. 1996. The crystal structure of the DNA-binding domain of yeast RAP1 in complex with telomeric DNA. *Cell.* 85:125–136. doi:10.1016/S0092-8674(00)81088-0

Kuzmichev, A., R. Margueron, A. Vaquero, T.S. Preissner, M. Scher, A. Kirmizis, X. Ouyang, N. Brockdorff, C. Abate-Shen, P. Farnham, and D. Reinberg. 2005. Composition and histone substrates of polycomb repressive group complexes change during cellular differentiation. *Proc. Natl. Acad. Sci. USA.* 102:1859–1864. doi:10.1073/pnas.0409875102

Lagouge, M., C. Argmann, Z. Gerhart-Hines, H. Meziane, C. Lerin, F. Daussin, N. Messadeq, J. Milne, P. Lambert, P. Elliott, et al. 2006. Resveratrol improves mitochondrial function and protects against metabolic disease by activating SIRT1 and PGC-1alpha. *Cell.* 127:1109–1122. doi:10.1016/j.cell.2006.11.013

Law, I.K., L. Liu, A. Xu, K.S. Lam, P.M. Vanhoutte, C.M. Che, P.T. Leung, and Y. Wang. 2009. Identification and characterization of proteins interacting with SIRT1 and SIRT3: implications in the anti-aging and metabolic effects of sirtuins. *Proteomics.* 9:2444–2456. doi:10.1002/pmic.200800738

Li, B., S. Oestreich, and T. de Lange. 2000. Identification of human Rap1: implications for telomere evolution. *Cell.* 101:471–483. doi:10.1016/S0092-8674(00)80858-2

Li, K., A. Casta, R. Wang, E. Lozada, W. Fan, S. Kane, Q. Ge, W. Gu, D. Orren, and J. Luo. 2008. Regulation of WRN protein cellular localization and enzymatic activities by SIRT1-mediated deacetylation. *J. Biol. Chem.* 283:7590–7598. doi:10.1074/jbc.M709707200

Liang, F., S. Kume, and D. Koya. 2009. SIRT1 and insulin resistance. *Nat. Rev. Endocrinol.* 5:367–373. doi:10.1038/nrendo.2009.101

Lim, D.S., S.T. Kim, B. Xu, R.S. Maser, J. Lin, J.H. Petrini, and M.B. Kastan. 2000. ATM phosphorylates p95/nbs1 in an S-phase checkpoint pathway. *Nature.* 404:613–617. doi:10.1038/35007091

Liu, D., M.S. O'Connor, J. Qin, and Z. Songyang. 2004. Telosome, a mammalian telomere-associated complex formed by multiple telomeric proteins. *J. Biol. Chem.* 279:51338–51342. doi:10.1074/jbc.M409293200

Marión, R.M., K. Strati, H. Li, M. Murga, R. Blanco, S. Ortega, O. Fernandez-Capetillo, M. Serrano, and M.A. Blasco. 2009a. A p53-mediated DNA damage response limits reprogramming to ensure iPS cell genomic integrity. *Nature.* 460:1149–1153. doi:10.1038/nature08287

Marion, R.M., K. Strati, H. Li, A. Tejera, S. Schoeftner, S. Ortega, M. Serrano, and M.A. Blasco. 2009b. Telomeres acquire embryonic stem cell characteristics in induced pluripotent stem cells. *Cell Stem Cell.* 4:141–154. doi:10.1016/j.stem.2008.12.010

Martínez, P., M. Thanasoula, P. Muñoz, C. Liao, A. Tejera, C. McNees, J.M. Flores, O. Fernández-Capetillo, M. Tarsounas, and M.A. Blasco. 2009. Increased telomere fragility and fusions resulting from TRF1 deficiency lead to degenerative pathologies and increased cancer in mice. *Genes Dev.* 23:2060–2075. doi:10.1101/gad.543509

McBurney, M.W., X. Yang, K. Jardine, M. Bieman, J. Th'ng, and M. Lemieux. 2003. The absence of SIR2alpha protein has no effect on global gene silencing in mouse embryonic stem cells. *Mol. Cancer Res.* 1:402–409.

McEachern, M.J., A. Krauskopf, and E.H. Blackburn. 2000. Telomeres and their control. *Annu. Rev. Genet.* 34:331–358. doi:10.1146/annurev.genet.34.1.331

Milne, J.C., P.D. Lambert, S. Schenk, D.P. Carney, J.J. Smith, D.J. Gagne, L. Jin, O. Boss, R.B. Perni, C.B. Vu, et al. 2007. Small molecule activators of SIRT1 as therapeutics for the treatment of type 2 diabetes. *Nature.* 450:712–716. doi:10.1038/nature06261

Milner, J. 2009. Cellular regulation of SIRT1. *Curr. Pharm. Des.* 15:39–44. doi:10.2174/138161209787185841

Muñoz, P., R. Blanco, J.M. Flores, and M.A. Blasco. 2005. XPF nuclease-dependent telomere loss and increased DNA damage in mice overexpressing TRF2 result in premature aging and cancer. *Nat. Genet.* 37:1063–1071. doi:10.1038/ng1633

Narala, S.R., R.C. Allsopp, T.B. Wells, G. Zhang, P. Prasad, M.J. Coussens, D.J. Rossi, I.L. Weissman, and H. Vaziri. 2008. SIRT1 acts as a nutrient-sensitive growth suppressor and its loss is associated with increased AMPK and telomerase activity. *Mol. Biol. Cell.* 19:1210–1219. doi:10.1091/mbc.E07-09-0965

Oberdoerffer, P., S. Michan, M. McVay, R. Mostoslavsky, J. Vann, S.K. Park, A. Hartlerode, J. Stegmuller, A. Hafner, P. Loerch, et al. 2008. SIRT1 redistribution on chromatin promotes genomic stability but alters gene expression during aging. *Cell.* 135:907–918. doi:10.1016/j.cell.2008.10.025

Ogami, M., Y. Ikura, M. Ohsawa, T. Matsuo, S. Kayo, N. Yoshimi, E. Hai, N. Shirai, S. Ehara, R. Komatsu, et al. 2004. Telomere shortening in human coronary artery diseases. *Arterioscler. Thromb. Vasc. Biol.* 24:546–550. doi:10.1161/01.ATV.0000117200.46938.e7

Ornish, D., J. Lin, J. Daubenmier, G. Weidner, E. Epel, C. Kemp, M.J. Magbanua, R. Marlin, L. Yglecias, P.R. Carroll, and E.H. Blackburn. 2008. Increased telomerase activity and comprehensive lifestyle changes: a pilot study. *Lancet Oncol.* 9:1048–1057. doi:10.1016/S1470-2045(08)70234-1

Panossian, L.A., V.R. Porter, H.F. Valenzuela, X. Zhu, E. Reback, D. Masterman, J.L. Cummings, and R.B. Effros. 2003. Telomere shortening in T cells correlates with Alzheimer's disease status. *Neurobiol. Aging.* 24:77–84. doi:10.1016/S0197-4580(02)00043-X

Park, M.J., Y.K. Jang, E.S. Choi, H.S. Kim, and S.D. Park. 2002. Fission yeast Rap1 homolog is a telomere-specific silencing factor and interacts with Taz1p. *Mol. Cells.* 13:327–333.

Pearson, K.J., J.A. Baur, K.N. Lewis, L. Peshkin, N.L. Price, N. Labinskyy, W.R. Swindell, D. Kamara, R.K. Minor, E. Perez, et al. 2008. Resveratrol delays age-related deterioration and mimics transcriptional aspects of dietary restriction without extending life span. *Cell Metab.* 8:157–168. doi:10.1016/j.cmet.2008.06.011

Perrod, S., and S.M. Gasser. 2003. Long-range silencing and position effects at telomeres and centromeres: parallels and differences. *Cell. Mol. Life Sci.* 60:2303–2318. doi:10.1007/s00018-003-3246-x

Perry, P., and S. Wolff. 1974. New Giemsa method for the differential staining of sister chromatids. *Nature.* 251:156–158. doi:10.1038/251156a0

Pfluger, P.T., D. Herranz, S. Velasco-Miguel, M. Serrano, and M.H. Tschöp. 2008. Sirt1 protects against high-fat diet-induced metabolic damage. *Proc. Natl. Acad. Sci. USA.* 105:9793–9798. doi:10.1073/pnas.0802917105

Potts, P.R., and H. Yu. 2007. The SMC5/6 complex maintains telomere length in ALT cancer cells through SUMOylation of telomere-binding proteins. *Nat. Struct. Mol. Biol.* 14:581–590. doi:10.1038/nsmb1259

Prozorovski, T., U. Schulze-Topphoff, R. Glumm, J. Baumgart, F. Schröter, O. Ninnemann, E. Siegert, I. Bendix, O. Brüstle, R. Nitsch, et al. 2008. Sirt1 contributes critically to the redox-dependent fate of neural progenitors. *Nat. Cell Biol.* 10:385–394. doi:10.1038/ncb1700

Rine, J., J.N. Strathern, J.B. Hicks, and I. Herskowitz. 1979. A suppressor of mating-type locus mutations in *Saccharomyces cerevisiae*: evidence for and identification of cryptic mating-type loci. *Genetics.* 93:877–901.

Rusin, M., A. Zajkowicz, and D. Butkiewicz. 2009. Resveratrol induces senescence-like growth inhibition of U-2 OS cells associated with the instability of telomeric DNA and upregulation of BRCA1. *Mech. Ageing Dev.* 130:528–537. doi:10.1016/j.mad.2009.06.005

Samper, E., F.A. Goytisolo, P. Slijepcevic, P.P. van Buul, and M.A. Blasco. 2000. Mammalian Ku86 protein prevents telomeric fusions independently of the length of TTAGGG repeats and the G-strand overhang. *EMBO Rep.* 1:244–252. doi:10.1093/embo-reports/kvd051

Saunders, L.R., and E. Verdin. 2009. Cell biology. Stress response and aging. *Science.* 323:1021–1022. doi:10.1126/science.1170007

Saunders, L.R., A.D. Sharma, J. Tawney, M. Nakagawa, K. Okita, S. Yamanaka, H. Willenbring, and E. Verdin. 2010. miRNAs regulate SIRT1 expression during mouse embryonic stem cell differentiation and in adult mouse tissues. *Aging (Albany NY).* 2:415–431.

Schoeftner, S., and M.A. Blasco. 2008. Developmentally regulated transcription of mammalian telomeres by DNA-dependent RNA polymerase II. *Nat. Cell Biol.* 10:228–236. doi:10.1038/ncb1685

Schotta, G., M. Lachner, K. Sarma, A. Ebert, R. Sengupta, G. Reuter, D. Reinberg, and T. Jenuwein. 2004. A silencing pathway to induce H3-K9 and H4-K20 trimethylation at constitutive heterochromatin. *Genes Dev.* 18:1251–1262. doi:10.1101/gad.300704

Sfeir, A., S.T. Kosiyatrakul, D. Hockemeyer, S.L. MacRae, J. Karlseder, C.L. Schildkraut, and T. de Lange. 2009. Mammalian telomeres resemble fragile sites and require TRF1 for efficient replication. *Cell.* 138:90–103. doi:10.1016/j.cell.2009.06.021

Sinclair, D.A., and L. Guarente. 1997. Extrachromosomal rDNA circles—a cause of aging in yeast. *Cell.* 91:1033–1042. doi:10.1016/S0092-8674(00)80493-6

Takai, H., A. Smogorzewska, and T. de Lange. 2003. DNA damage foci at dysfunctional telomeres. *Curr. Biol.* 13:1549–1556. doi:10.1016/S0960-9822(03)00542-6

Takai, K.K., S. Hooper, S. Blackwood, R. Gandhi, and T. de Lange. 2010. In vivo stoichiometry of shelterin components. *J. Biol. Chem.* 285:1457–1467. doi:10.1074/jbc.M109.038026

Tomás-Loba, A., I. Flores, P.J. Fernández-Marcos, M.L. Cayuela, A. Maraver, A. Tejera, C. Borrás, A. Matheu, P. Klatt, J.M. Flores, et al. 2008. Telomerase reverse transcriptase delays aging in cancer-resistant mice. *Cell.* 135:609–622. doi:10.1016/j.cell.2008.09.034

Uhl, M., A. Csernok, S. Aydin, R. Kreienberg, L. Wiesmüller, and S.A. Gatz. 2010. Role of SIRT1 in homologous recombination. *DNA Repair (Amst.).* 9:383–393. doi:10.1016/j.dnarep.2009.12.020

Vaitiekunaite, R., D. Butkiewicz, M. Krześniak, M. Przybyłek, A. Gryc, M. Snietura, M. Benedyk, C.C. Harris, and M. Rusin. 2007. Expression and localization of Werner syndrome protein is modulated by SIRT1 and PML. *Mech. Ageing Dev.* 128:650–661. doi:10.1016/j.mad.2007.09.004

Valdes, A.M., T. Andrew, J.P. Gardner, M. Kimura, E. Oelsner, L.F. Cherkas, A. Aviv, and T.D. Spector. 2005. Obesity, cigarette smoking, and telomere length in women. *Lancet.* 366:662–664. doi:10.1016/S0140-6736(05)66630-5

Vaquero, A., M. Scher, D. Lee, H. Erdjument-Bromage, P. Tempst, and D. Reinberg. 2004. Human SirT1 interacts with histone H1 and promotes formation of facultative heterochromatin. *Mol. Cell.* 16:93–105. doi:10.1016/j.molcel.2004.08.031

Vaquero, A., M. Scher, H. Erdjument-Bromage, P. Tempst, L. Serrano, and D. Reinberg. 2007. SIRT1 regulates the histone methyl-transferase SUV39H1 during heterochromatin formation. *Nature.* 450:440–444. doi:10.1038/nature06268

Wang, F., M. Nguyen, F.X. Qin, and Q. Tong. 2007. SIRT2 deacetylates FOXO3a in response to oxidative stress and caloric restriction. *Aging Cell.* 6:505–514. doi:10.1111/j.1474-9726.2007.00304.x

Wang, R.H., K. Sengupta, C. Li, H.S. Kim, L. Cao, C. Xiao, S. Kim, X. Xu, Y. Zheng, B. Chilton, et al. 2008. Impaired DNA damage response, genome instability, and tumorigenesis in SIRT1 mutant mice. *Cancer Cell.* 14:312–323. doi:10.1016/j.ccr.2008.09.001

Westerheide, S.D., J. Anckar, S.M. Stevens Jr., L. Sistonen, and R.I. Morimoto. 2009. Stress-inducible regulation of heat shock factor 1 by the deacetylase SIRT1. *Science.* 323:1063–1066. doi:10.1126/science.1165946

Wood, J.G., B. Rogina, S. Lavu, K. Howitz, S.L. Helfand, M. Tatar, and D. Sinclair. 2004. Sirtuin activators mimic caloric restriction and delay ageing in metazoans. *Nature.* 430:686–689. doi:10.1038/nature02789

Xu, F., Q. Zhang, K. Zhang, W. Xie, and M. Grunstein. 2007. Sir2 deacetylates histone H3 lysine 56 to regulate telomeric heterochromatin structure in yeast. *Mol. Cell.* 27:890–900. doi:10.1016/j.molcel.2007.07.021

Yamazaki, Y., I. Usui, Y. Kanatani, Y. Matsuya, K. Tsuneyama, S. Fujisaka, A. Bukhari, H. Suzuki, S. Senda, S. Imanishi, K. Hirata, M. Ishiki, R. Hayashi, M. Urakaze, H. Nemoto, M. Kobayashi, and K. Tobe. 2009. Treatment with SRT1720, a SIRT1 activator, ameliorates fatty liver with reduced expression of lipogenic enzymes in MSG mice. *Am. J. Physiol. Endocrinol. Metab.* doi: 10.1152/ajpendo.90997.2008

Yuan, Z., and E. Seto. 2007. A functional link between SIRT1 deacetylase and NBS1 in DNA damage response. *Cell Cycle.* 6:2869–2871. doi:10.4161/cc.6.23.5026

Yuan, Z., X. Zhang, N. Sengupta, W.S. Lane, and E. Seto. 2007. SIRT1 regulates the function of the Nijmegen breakage syndrome protein. *Mol. Cell.* 27:149–162. doi:10.1016/j.molcel.2007.05.029

Zijlmans, J.M., U.M. Martens, S.S. Poon, A.K. Raap, H.J. Tanke, R.K. Ward, and P.M. Lansdorp. 1997. Telomeres in the mouse have large inter-chromosomal variations in the number of T2AG3 repeats. *Proc. Natl. Acad. Sci. USA.* 94:7423–7428. doi:10.1073/pnas.94.14.7423